IOWA STATE UNIVERSITY
Digital Repository

Graduate Theses and Dissertations

Iowa State University Capstones, Theses and Dissertations

2010

A novel and cost-effective hydrogen sulfide removal technology using tire derived rubber particles

Andrea Mary Siefers
Iowa State University

Follow this and additional works at: https://lib.dr.iastate.edu/etd

 Part of the Civil and Environmental Engineering Commons

Recommended Citation
Siefers, Andrea Mary, "A novel and cost-effective hydrogen sulfide removal technology using tire derived rubber particles" (2010). *Graduate Theses and Dissertations*. 11281.
https://lib.dr.iastate.edu/etd/11281

This Thesis is brought to you for free and open access by the Iowa State University Capstones, Theses and Dissertations at Iowa State University Digital Repository. It has been accepted for inclusion in Graduate Theses and Dissertations by an authorized administrator of Iowa State University Digital Repository. For more information, please contact digirep@iastate.edu.

www.manaraa.com

A novel and cost-effective hydrogen sulfide removal technology using tire derived rubber particles

by

Andrea Mary Siefers

A thesis submitted to the graduate faculty

in partial fulfillment of the requirements for the degree of

MASTER OF SCIENCE

Major: Civil Engineering (Environmental Engineering)

Program of Study Committee:

Timothy G. Ellis, Major Professor
Hans van Leeuwen
Michael (Hogan) Martin

Iowa State University

Ames, Iowa

2010

Copyright © Andrea Mary Siefers, 2010. All rights reserved.

www.manaraa.com

TABLE OF CONTENTS

www.manaraa.com

www.manaraa.com

www.manaraa.com

LIST OF FIGURES

www.manaraa.com

LIST OF TABLES

www.manaraa.com

ABSTRACT

Hydrogen sulfide (H_2S) is corrosive, toxic, and produced during the anaerobic digestion process at wastewater treatment plants. Tire derived rubber particles (TDRP™) and other rubber material (ORM™) are recycled waste rubber products distributed by Envirotech Systems, Inc (Lawton, IA). They were found to be effective at removing H_2S from biogas in a previous study. A scrubber system utilizing TDRP™ and ORM™ was tested at the Ames Water Pollution Control Facility (WPCF) to determine operational conditions that would optimize the amount of H_2S removed from biogas in order to allow for systematic sizing of biogas scrubbers.

Operational conditions tested were empty bed contact time, mass of the media bed, compaction of the media bed, and temperature of the biogas and scrubber media. Additionally, siloxane concentrations were tested before and after passing through the scrubber. The two different types of products, TDRP™ and ORM™, differed in metal concentrations and particle size distribution. A scrubber system was set up and maintained in the Gas Handling Building at the WPCF from February to December 2009.

Results showed that longer contact times, compaction, and higher inlet H_2S concentrations improved the amount of H_2S that was adsorbed by the TDRP™ and ORM™. The inlet H_2S concentration of the biogas was found to be variable over time and was affected by large additions of fats, oils, and grease (FOG). The effect of temperature was not found to be significant. In excess of 98% siloxane reduction was observed from the biogas.

The Freundlich Isotherm was successfully fit to experimental data at ambient temperatures (near 25°C) and low temperatures (14-20°C). Using assumptions about the concentration of H_2S, flow of biogas, and temperature at the WPCF, it was found that the volume of ORM™ and TDRP™ needed for one year of H_2S removal at the WPCF at 25°C would be approximately 12.48 m^3 and 6.77 m^3, respectively.

www.manaraa.com

CHAPTER 1. INTRODUCTION

Biogas, produced by the decomposition of organic matter, is becoming an important source of energy. Biogas is released due to anthropogenic activities from landfills, commercial composting, anaerobic digestion of wastewater sludge, animal farm manure anaerobic fermentation, and agrifood industry sludge anaerobic fermentation. Biogas contains methane (CH_4), which has a high energy value, and is increasingly being used as an energy source (Abatzoglou & Boivin, 2009). A compound in biogas, hydrogen sulfide (H_2S), is corrosive, toxic, and odorous. This study focuses on biogas produced by the anaerobic digestion of wastewater sludge. Biogas from anaerobic processes at wastewater treatment plants can contain up to 2,000 ppm H_2S (Osorio & Torres, 2009). Exposure to hydrogen sulfide can be acutely fatal at concentrations between 500 and 1,000 ppm or higher, and the maximum allowable daily exposure without appreciable risk of deleterious effects during a lifetime is 1.4 ppb (U.S. EPA, 2003), although OSHA regulations allow concentrations up to 10 ppm for prolonged exposure (Nagl, 1997). Hydrogen sulfide can significantly damage mechanical and electrical equipment used for process control, energy generation, and heat recovery. The combustion of hydrogen sulfide results in the release of sulfur dioxide, which is a problematic environmental gas emission. Adsorption onto various media and chemical scrubbing are common methods of H_2S removal from biogas and other gasses. However, the media and chemical solutions used are often expensive and difficult to dispose.

Siloxanes are another problematic constituent of biogas. Siloxanes are a group of chemical compounds that have silicon-oxygen bonds with hydrocarbon groups attached to the silicon atoms. They are present in many consumer products and volatilize during the anaerobic digestion process. When siloxanes are combusted, they produce microcrystalline silica, which causes problems with the functioning of energy generating equipment. Current siloxane removal systems are costly and are impractical for smaller scale operations. (Abatzoglou & Boivin, 2009)

In preliminary research (Ellis, Park, & Oh, 2008), it was found that recycled waste tire rubber products, distributed by Envirotech Systems, Inc. and dubbed tire derived rubber particles (TDRP^{TM}) and other rubber material (ORM^{TM}) , were effective at adsorbing hydrogen sulfide. Billions of used tires and rubber products are discarded annually, and therefore waste rubber products are affordable and plentiful.

Presently, there are no existing studies which examine the ability or effectiveness of using polymeric materials such as rubber as media for scrubbing biogas. Current studies focus on other

www.manaraa.com

materials, such as activated carbon, zeolites, metal oxides, or sludge-derived products as adsorbents, or on other applications of waste tire rubber.

Project Objectives

The objective of this study was to find operational conditions that would maximize the amount of hydrogen sulfide removed from biogas in order to allow for systematic sizing of biogas scrubbers using TDRP and ORM. In addition to studying H_2S removal, changes in siloxane concentrations after biogas contact with TDRP were evaluated.

Using the biogas produced by the anaerobic digesters at the Ames Water Pollution Control Facility (WPCF), various conditions were tested to determine the optimal design and operational conditions for H_2S removal from the biogas. The following conditions were tested:

- Empty bed contact time
- Mass of TDRP used in the media bed
- Compaction of the media bed
- Temperature of the biogas and scrubber media

www.manaraa.com

CHAPTER 2. LITERATURE REVIEW

Characteristics of Biogas

Biogas produced from anaerobic processes is primarily composed of methane (CH_4) and carbon dioxide (CO_2), with smaller amounts of hydrogen sulfide (H_2S), ammonia (NH_3), hydrogen (H_2), nitrogen (N_2), carbon monoxide (CO), saturated or halogenated carbohydrates, and oxygen (O_2). Biogas is usually water saturated and also may contain dust particles and siloxanes (Wheeler, Jaatinen, Lindberg, Holm-Nielsen, Wellinger, & Pettigrew, 2000). The composition of biogas produced from anaerobic digestion at wastewater treatment plants is typically between 60 and 70 vol% CH_4, between 30 and 40 vol% CO_2, less than 1 vol% N_2, and between 10 and 2000 ppm H_2S (Osorio & Torres, 2009). Biogas has a higher heating value (HHV) between 15 and 30 MJ/Nm^3 (Abatzoglou & Boivin, 2009).

This review will focus on biogas produced from anaerobic digestion processes at wastewater treatment plants. Sewage sludge, which serves as the feedstock for these anaerobic digesters, contains sulfur-based compounds. Sulfates are the predominant form of sulfur in secondary sludge. During sludge thickening processes the sulfates begin to be converted into sulfides, due to the decreased amount of oxygen in the sludge caused by increased microbial activity. After anaerobic digestion, the oxidation-reduction potential of the sludge has decreased so much that all inorganic sulfur is transformed into sulfides. (Osorio & Torres, 2009)

Hydrogen sulfide is extremely toxic, corrosive, and odorous. It can be very problematic in the conversion of biogas to energy, as discussed in the next section. Some physical and chemical properties of hydrogen sulfide are listed in Table 1.

Table 1, Physical and chemical properties of hydrogen sulfide (U.S. EPA, 2003)

Molecular formula	H_2S
Molecular weight	34.08 g
Vapor pressure	15,600 mm Hg at 25°C
Density	1.5392 g/L at 0°C, 760 mm Hg
Boiling point	-60.33°C
Water solubility	3980 mg/L at 20°C
Dissociation constants	pKa1 = 7.04; pKa2 = 11.96
Conversion factor	1 ppm = 1.39 mg/m^3

www.manaraa.com

Siloxanes are also a problematic constituent in biogas. They are widely used in various industries due to their low flammability, low surface tension, thermal stability, hydrophobicity, high compressibility, low toxicity, ability to break down in the environment, and low allergenicity. They are increasingly found in shampoos, pressurized cans, detergents, cosmetics, pharmaceuticals, textiles, and paper coatings (Abatzoglou & Boivin, 2009). Siloxanes do not decompose during anaerobic digestion and instead are volatilized and exit the anaerobic digestion process with the biogas. Siloxanes form microcrystalline silica when oxidized, which is problematic in energy generation from biogas. There are two types of siloxanes that compose over 90% of total siloxanes in biogas: D4 (octamethylcyclotetrasiloxane, $C_8H_{24}O_4Si_4$) and D5 (decamethylcyclopentasiloxane, $C_{10}H_{30}O_5Si_5$). One study found an average concentration of approximately 28 mg/m^3 of D4 and D5 siloxanes in digester biogas with a maximum concentration of 122 mg/m^3 (McBean, 2008).

Biogas for Energy Generation

Due to the high fraction of methane, biogas can be utilized for energy generation. However, because of the contaminants present in biogas, it cannot always be substituted for natural gas in energy generation equipment. Boilers, which generate heat from gas, do not have a high gas quality requirement, although it is recommended that H_2S concentrations be kept below 1,000 ppm. It is recommended that the raw gas be condensed in order to remove water, which can potentially cause problems in the gas nozzles. Additionally, stainless steel, plastic, or other corrosion-resistant parts are recommended for the boilers, due to the high corrosivity and high temperatures that result from the condensation and combustion of biogas containing H_2S. (Wheeler et al., 2000)

Internal combustion engines, used for electricity generation, have comparable gas quality requirements to boilers. However, some types of engines are more susceptible to H_2S than others. Because of this, diesel engines are recommended for large scale energy conversion operations (>60 kW) (Wheeler et al., 2000). An additional problem posed by biogas in combustion engines are the formation of abrasive, silica based particles that are generated when siloxanes present in biogas combust. These particles can cause abrasion of metal surfaces, which can in turn cause ill-functioning spark plugs, overheating of sensitive parts of engines due to coating, and the general deterioration of all mechanical engine parts (Abatzoglou & Boivin, 2009).

www.manaraa.com

Biogas can also be utilized as a vehicle fuel. There are more than a million natural gas vehicles in the world. However, to use biogas in these vehicles, it must be upgraded because vehicles need a much higher gas quality. Carbon dioxide, hydrogen sulfide, ammonia, particulates, and water must be removed from the biogas, so that the methane content of the gas is at least 95 vol%. (Wheeler et al., 2000)

Methods of Controlling H_2S Emissions

Hydrogen sulfide produced industrially can be controlled using a variety of methods. Some of the methods can be used in combination. Some of the methods discussed are more commonly used in specific industrial processes. The process chosen is based on the end-use of the gas, the gas composition and physical characteristics, and the amount of gas that needs to be treated. Hydrogen sulfide removal processes can be either physical-chemical or biological.

Claus process

The Claus process is used in oil and natural gas refining facilities and removes H_2S by oxidizing it to elemental sulfur. The following reactions occur in various reactor vessels and the removal efficiency depends on the number of catalytic reactors used:

$$H_2S + 3/2O_2 \rightarrow SO_2 + H_2O \quad \text{(Eq. 1)}$$

$$2H_2S + SO_2 \rightarrow 3S^0 + 2H_2O \quad \text{(Eq. 2)}$$

$$H_2S + 1/2O_2 \rightarrow S^0 + H_2O \quad \text{(Eq. 3)}$$

Removal efficiency is about 95% using two reactors, and 98% using four reactors.

The ratio of O_2-to-H_2S must be strictly controlled to avoid excess SO_2 emissions or low H_2S removal efficiency. Therefore, the Claus process is most effective for large, consistent, acid gas streams (greater than 15 vol% H_2S concentration). When used for appropriate gas streams, Claus units can be highly effective at H_2S removal and also at producing high-purity sulfur. (Nagl, 1997)

Chemical oxidants

Chemical oxidants are most often used at wastewater treatment plants to control both odor and the toxic potential of H_2S. The systems are also often designed to remove other odor causing compounds produced during anaerobic processes. The most widely used chemical oxidation system

www.manaraa.com

is a combination of sodium hydroxide (NaOH) and sodium hypochlorite (NaOCl), which are chosen for their low cost, availability, and oxidation capability. Oxidation occurs by the following reactions:

$$H_2S + 2NaOH \leftrightarrow Na_2S + 2H_2O \quad \text{(Eq. 4)}$$

$$Na_2S + 4NaOCl \rightarrow Na_2SO_4 + 4NaCl \quad \text{(Eq. 5)}$$

The oxidants are continuously used in the process and therefore they provide an operating cost directly related to the amount of H_2S in the stream. This process is only economically feasible for gas streams with relatively low concentrations of H_2S. The gas phase must be converted to the liquid phase, as the reactions occur in the aqueous phase in the scrubber. Countercurrent packed columns are the most common type of scrubber, but other designs such as spray chambers, mist scrubbers, and venturis are also sometimes used. The products of the above reactions stay dissolved in the scrubber solution until the solution is saturated. To avoid salt precipitation, the scrubber solution is either continuously or periodically removed and replenished. (Nagl, 1997)

Caustic scrubbers

Caustic scrubbers function similarly to chemical oxidation systems, except that caustic scrubbers are equilibrium limited, meaning that if caustic is added, H_2S is removed, and if the pH decreases and becomes acidic, H_2S is produced. The following equation describes the caustic scrubber reaction:

$$H_2S + 2NaOH \leftrightarrow Na_2S + 2H_2O \quad \text{(Eq. 6)}$$

In a caustic scrubber, the pH is kept higher than 9 by continuously adding sodium hydroxide (NaOH). A purge stream must be added to prevent salt precipitation. However, if the purge stream is added back to other process streams, the reaction is pushed towards the left and H_2S is released. For this reason, the spent caustic must be carefully disposed. Additionally, the caustics are non-regenerable. (Nagl, 1997)

Adsorption

An adsorbing material can attract molecules in an influent gas stream to its surface. This removes them from the gas stream. Adsorption can continue until the surface of the material is covered and then the materials must either be regenerated (undergo desorption) or replaced. Regeneration processes can be both expensive and time consuming. Activated carbon is often used

www.manaraa.com

for the removal of H_2S by adsorption. Activated carbon can be impregnated with potassium hydroxide (KOH) or sodium hydroxide (NaOH), which act as catalysts to remove H_2S. Activated carbon and other materials used for adsorption are discussed in detail in a later section. (Nagl, 1997)

H_2S scavengers

Hydrogen sulfide scavengers are chemical products that react directly with H_2S to create innocuous products. Some examples of H_2S scavenging systems are: caustic and sodium nitrate solution, amines, and solid, iron-based adsorbents. These systems are sold under trademarks by various companies. The chemical products are applied in columns or sprayed directly into gas pipelines. Depending on the chemicals used, there will be various products of the reactions. Some examples are elemental sulfur and iron sulfide (FeS_2). (Nagl, 1997)

One commercially available H_2S scavenging system using chelated iron H_2S removal technology is the LO-CAT®(US Filter/Merichem) process. It can remove more than 200 kg of S/day and is ideal for landfill gas. (Abatzoglou & Boivin, 2009)

Amine absorption units

Alkanolamines (amines) are both water soluble and have the ability to absorb acid gases. This is due to their chemical structure, which has one hydroxyl group and one amino group. Amines are able to remove H_2S by absorbing them, and then dissolving them in an aqueous amine stream. The stream is then heated to desorb the acidic components, which creates a concentrated gas stream of H_2S, which can then be used in a Claus unit or other unit to be converted to elemental sulfur. This process is best used for anaerobic gas streams because oxygen can oxidize the amines, limiting the efficiency and causing more material to be used (Nagl, 1997). Amines that are commonly used are monoethanolamine (MEA), diethanolamine (DEA), and methyldiethanolamine (MDEA).

Amine solutions are most commonly used in natural-gas purification processes. They are attractive because of the potential for high removal efficiencies, their ability to be selective for either H_2S or both CO_2 and H_2S removal, and are regenerable (McKinsey Zicarai, 2003). One problem associated with this process is that a portion of the amine gas is either lost or degraded during H_2S removal and it is expensive and energy intensive to regenerate or replace the solution (Wang, Ma,

www.manaraa.com

Xu, Sun, & Song, 2008). Other disadvantages include complicated flow schemes, foaming problems, and how to dispose of foul regeneration air (McKinsey Zicarai, 2003).

Liquid-phase oxidation systems

Liquid-phase oxidation systems convert H_2S into elemental sulfur through redox reactions by electron transfer from sources such as vanadium or iron reagents. The Stretford process is regarded as the first liquid-phase oxidation system. Hydrogen sulfide is first absorbed into an aqueous, alkali solution. It is then oxidized to elemental sulfur, while the vanadium reagent is reduced. This process is relatively slow and usually occurs in packed columns or venturis. However, vanadium is toxic and these units must be designed so that both the "sulfur cake" and solution are cleaned. (Nagl, 1997)

Because of problems with the Stretford process, liquid-phase oxidation systems have now been designed using iron-based reagents. Chelating agents are used to increase iron solubility in water so that liquid streams, as well as gas phases, can be treated. Ferric iron is reduced to ferrous iron in the process, while hydrogen sulfide is oxidized to elemental sulfur (Nagl, 1997). Ferrous iron (Fe^{2+}) can be regenerated by air oxidation (Abatzoglou & Boivin, 2009). The reaction between the hydrogen sulfide and iron occurs much faster than in the Stretford process (Nagl, 1997). One system, LO-CAT® by US Filter/Merichem, is an example of a H_2S removal system that utilizes chelated iron solution. The basic reactions are as shown in Eq. 7 and 8:

$$2Fe^{3+} + H_2S \rightarrow 2Fe^{2+} + S + 2H^{+} \qquad \text{(Eq. 7)}$$

$$2Fe^{2+} + \tfrac{1}{2}\, O_2 + H_2O \rightarrow 2Fe^{3+} + 2OH^{-} \qquad \text{(Eq. 8)}$$

The LO-CAT® system is attractive for H_2S removal from biogas streams because it is over 99% effective, the catalyst solution is non-toxic, and it can operate at ambient temperatures. (McKinsey Zicarai, 2003)

Other metal-based reagents can also be used. Magnesium and copper sulfate solutions have been tested, but due to the complexity, costs, and severity of reactions, it is unlikely that these reagents can be utilized for hydrogen sulfide removal from biogas. (Abatzoglou, Boivin, 2009).

Physical solvents

Using physical solvents as a method to remove acid gases, such as H_2S, can be economical depending on the end use of the gas. Hydrogen sulfide can be dissolved in a liquid and then later

www.manaraa.com

removed from the liquid by reducing the pressure. For more effective removal, liquids with higher solubility for H_2S are used. However, water is widely available and low-cost. Water washing is one example of a physical solvent-utilizing process. Water also has solubility potential for CO_2, and selective removal of just H_2S has not proved economical using water. (McKinsey Zicarai, 2003)

Other physical solvents that have been used are methanol, propylene carbonate, and ethers of polyethylene glycol. Criteria for selecting a physical solvent are high absorption capacity, low reactivity with equipment and gas constituents, and low viscosity. One problem with using physical solvents is that a loss of product usually occurs, due to the pressure changing processes necessary to later remove the H_2S from the solvent. Losses as high as 10% have been found. (McKinsey Zicarai, 2003).

Membrane processes

Membranes can be used to purify biogas. Partial pressures on either side of the membrane control permeation through the membrane. Membranes are not usually used for selective removal of H_2S, and are rather used to upgrade biogas to natural gas standards. There are two types of membrane systems: high pressure with gas phase on both sides of the membrane, and low pressure with a liquid adsorbent on one side. In one case, cellulose acetate membranes were used to upgrade biogas produced by anaerobic digesters. (McKinsey Zicarai, 2003)

Biological methods

Microorganisms have been used for the removal of H_2S from biogas. Ideal microorganisms would have the ability to transform H_2S to elemental sulfur, could use CO_2 as their carbon source (eliminating a need for nutrient input), could produce elemental sulfur that is easy to separate from the biomass, would avoid biomass accumulation to prevent clogging problems, and would be able to withstand a variety of conditions (fluctuation in temperature, moisture, pH, O_2/H_2S ratio, for example). Chemotrophic bacterial species, particularly from the Thiobacillus genus, are commonly used. Chemotrophic thiobacteria can be used both aerobically and anaerobically. They can utilize CO_2 as a carbon source and use chemical energy from the oxidation of reduced inorganic compounds, such as H_2S. In both reactions, H_2S first dissociates:

$$H_2S \leftrightarrow H^+ + HS^- \qquad \text{(Eq. 9)}$$

Under limited oxygen conditions, elemental sulfur is produced:

www.manaraa.com

$$HS^- + 0.5O_2 \rightarrow S^0 + OH^- \quad \text{(Eq. 10)}$$

Under excess oxygen conditions, SO_4^{2-} is produced, which leads to acidification:

$$HS^- + 2O_2 \rightarrow SO_4^{2-} + H^+ \quad \text{(Eq. 11)}$$

One chemotrophic aerobe, *Thiobacillus ferroxidans*, removes H_2S by oxidizing $FeSO_4$ to $Fe_2(SO_4^{2-})_3$, and then the resulting Fe^{3+} solution can dissolve H_2S and chemically oxidize it to elemental sulfur. These bacteria are also able to grow at low pH levels, which make them easy to adapt to highly fluctuating systems. (Abatzoglou & Boivin, 2009)

Biological H_2S removal can be utilized in biofilter and bioscrubber designs. One commercially available biological H_2S removal system is Thiopaq®. It uses chemotrophic thiobacteria in an alkaline environment to oxidize sulfide to elemental sulfur. It is able to simultaneously regenerate hydroxide, which is used to dissociate H_2S. Flows can be from 200 Nm^3/h to 2,500 Nm^3/h and up to 100% H_2S, with outlet concentrations of below 4 ppmv. (Abatzoglou & Boivin, 2009)

Another system, H_2SPLUS SYSTEM®, uses both chemical and biological methods to remove H_2S. A filter consisting of iron sponge inoculated with thiobacteria is used. There are about 30 systems currently in use in the U.S., mostly at agrifood industry wastewater treatment plants. Gas flows of 17 to 4,200 m^3/h can be used, and removal capacity is up to 225 kg H_2S/day. (Abatzoglou & Boivin, 2009)

Materials Used for H_2S Adsorption

Various materials are used as adsorbents for hydrogen sulfide. These materials have specific surface properties, chemistry, and other factors that make them useful as H_2S adsorbents. A study by Yan, Chin, Ng, Duan, Liang, and Tay (2004) about mechanisms of H_2S adsorption revealed that H_2S is first removed by physical adsorption onto the liquid water film on the surface of the adsorbent, then by the dissociation of H_2S and the HS^- reaction with metal oxides to form sulfides, then with alkaline species to give neutralization products, and finally with surface oxygen species to give redox reaction products (such as elemental sulfur). If water is not present, CO_2 can deactivate the alkaline-earth-metal-based reaction sites and lead to lower H_2S removal. Additionally, the oxidation reactions of H_2S are faster when Ca, Mg, and Fe are present, as they are catalysts for these reactions (Abatzoglou & Boivin, 2009). Physical adsorption also occurs in pores, and pores between the size of

www.manaraa.com

0.5 and 1 nm were found by Yan et al. to have the best adsorption capacity. Significant adsorption occurs when a material is able to sustain multiple mechanisms. The materials described in this section have been shown to utilize one or more of these mechanisms and have shown potential as H_2S adsorbent materials.

Activated carbon

Activated carbons are frequently used for gas adsorption because of their high surface area, porosity, and surface chemistry where H_2S can be physically and chemically adsorbed (Yuan & Bandosz, 2007). Much of the research has focused on how the physical and chemical properties of various activated carbons affect the breakthrough capacity of H_2S. Most activated carbon tested is in granular form, called Granular Activated Carbon (GAC). Activated carbon can come in two forms: unimpregnated and impregnated. Impregnation refers to the addition of cations to assist as catalysts in the adsorption process (Bandosz, 2002). Unimpregnated activated carbon removes hydrogen sulfide at a much slower rate because activated carbon is only a weak catalyst and is rate-limited by the complex reactions that occur. However, using low H_2S concentrations and given sufficient time, removal capacities of impregnated and unimpreganted activated appear to be comparable in laboratory tests. Removal capacities may vary greatly in on-site applications, as the presence of other constituents (such as VOCs) may inhibit or enhance the removal capacity, depending on other environmental conditions (Bandosz, 2002). The cations added to impregnated activated carbon are usually caustic compounds such as sodium hydroxide (NaOH) or potassium hydroxide (KOH), which act as strong bases that react with H_2S and immobilize it. Other compounds used to impregnate activated carbons are sodium bicarbonate ($NaHCO_3$), sodium carbonate (Na_2CO_3), potassium iodide (KI), and potassium permanganate ($KMnO_4$)(Abatzoglou & Boivin, 2009). When caustics are used, the activated carbon acts more as a passive support for the caustics rather than actively participating in the H_2S removal because of its low catalytic ability. The caustic addition has a catalytic effect by oxidizing the sulfide ions to elemental sulfur until there is no caustic left to react. The reactions that unimpregnated activated carbon undergoes to facilitate H_2S removal is far less understood (Bandosz, 2002). A typical H_2S adsorption capacity for impregnated activated carbons is 150 mg H_2S/g of activated carbon. A typical H_2S adsorption capacity for unimpregnated activated carbons is 20 mg H_2S/g of activated carbon. (Abatzoglou & Boivin, 2009)

www.manaraa.com

Much research has focused on mechanisms of H_2S removal using activated carbon. A researcher from the Department of Chemistry in the City College of New York, Teresa Bandosz, has performed numerous studies on the adsorption of H_2S on activated carbons (Bandosz, 2002; Adib, Bagreev, & Bandosz, 2000; Bagreev & Bandosz, 2002; Bagreev, Katikaneni, Parab, & Bandosz, 2005; Yuan & Bandosz, 2007). Her studies have focused on hydrogen sulfide adsorption on activated carbons as it relates to surface properties, surface chemistry, temperature, concentration of H_2S gas, addition of cations, moisture of gas stream, and pH. These experiments have used both biogas from real processes and laboratory produced gases of controlled composition.

In a study by Bagreev and Bandosz (2002), NaOH impregnated activated carbon was tested for its H_2S removal capacity. Four different types of activated carbon were used and different volume percentages of NaOH were added. The results showed that with increasing amounts of NaOH added, the H_2S removal capacity of the activated carbons increases. This effect occurred until maximum capacity was reached at 10 vol% NaOH. This result was the same regardless of the origin of the activated carbon, and was even the same when activated alumina was used. This result implies that the amount of NaOH present on the surface of the material is a limiting factor for the H_2S removal capacity in NaOH impregnated activated carbons.

Although impregnated activated carbon can be an effective material for the adsorption of H_2S, there are a few drawbacks of using this material. First, the addition of caustics lowers the ignition temperature and therefore the material can self-ignite and is considered hazardous. Secondly, the addition of caustics to activated carbon increases the costs of production. Lastly, because of the high cost of activated carbon, it is desirable to "wash" or "clean" the activated carbon in order to regenerate it so that it will regain some of its ability to remove H_2S (Calgon Carbon Corp., a leading producer of activated carbon, priced an unimpregnated activated carbon used in wastewater treatment applications to be $8.44/lb and impregnated activated carbon is even more expensive). One of the simple ways to regenerate the activated carbon is to wash it with water. The caustic additions to impregnated activated carbon cause H_2S to be oxidized to elemental sulfur, which cannot be removed from the activated carbon by washing with water and therefore costs of H_2S removal are increased due to the need to purchase more adsorbent. (Bandosz, 2002)

As of yet, the complete mechanisms by which H_2S is removed using activated carbon are not well understood. It is accepted that removal occurs by both physical and chemical mechanisms. One

www.manaraa.com

chemical removal mechanism is caused by the presence of heteroatoms at the carbon surface. Important heteroatoms are oxygen, nitrogen, hydrogen, and phosphorus. They are incorporated as functional groups in the carbon matrix and originate in the activated carbon as residuals from organic precursors and components in the agent used for chemical activation. They are important in the chemical removal of H_2S because they influence the pH of the carbon, which can control which species (acidic, basic, or polar) are chemisorbed at the surface. Another important factor in H_2S removal has been the presence of moisture on the carbon surface. Bandosz has a theory that, in unimpregnated activated carbon, H_2S will dissociate in the film of water at the carbon surface and the resulting sulfide ions (HS^-) are oxidized to elemental sulfur (Bandosz, 2002). Bandosz found that the activated carbon's affinity for water should not be greater than 5%, otherwise the small pores of the adsorbent become filled by condensed adsorbate and the direct contact of HS^- with the carbon surface becomes limited. It was found that some affinity for water adsorption was desirable in an adsorbent. However, when biogas is used at the source of H_2S, it is not practical to optimize the amount of water on the media because biogas is usually already water saturated. Too much water can interfere with the H_2S removal reactions because the water in gaseous form reacts with CO_2 to form carbonates and contributes to the formation of sulfurous acid which can deactivate the catalytic sites and reduce the capacity for hydrogen sulfide to react and be removed (Abatzoglou & Boivin, 2009).

Bandosz and her research group have focused considerably on the mechanisms of H_2S removal on unimpregnated activated carbon. In Adib, Bagreev, & Bandosz (2000) it was found that as oxidation occurs on the surface of the carbons, the capacity for adsorption decreases. The adsorption and immobilization of H_2S was found to be related to its ability to dissociate and this was inhibited by the oxidized surface of the activated carbons. No relationship between pore structure and adsorption ability was found, but it was noted that a higher volume of micropores with small volumes enhances the adsorption capacity. The most important finding of this study was that the pH of the surface has a large affect on the ability of H_2S to dissociate. Acidic surfaces (<5) decrease the H_2S adsorption capacity of the activated carbons.

The concentration of H_2S in the inlet gas may affect the adsorption capacity of activated carbons. One study indicated that the H_2S removal capacity of impregnated activated carbons increases when the H_2S concentration decreases (Bagreev et. al, 2005). In the same study, it was

www.manaraa.com

also found that small differences in oxygen content (1-2%) and different temperatures (from 38°C-60°C) did not have a significant effect on the hydrogen sulfide removal. In another study, it was found that adsorption capacities of H_2S on impregnated activated carbon slightly decrease with increasing temperature (30 and 60°C were tested). (Xiao, Ma, Xu, Sun, & Song, 2008)

The effect of low H_2S concentration on removal capacity can be explained by the fact that the low concentration slows down oxidation kinetics, which in turn slows down the rate of surface acidification. Surface acidification has been shown to be detrimental to H_2S removal because H_2S does not dissociate readily in acidic conditions (Abatzoglou & Boivin, 2009).

Zeolites (Molecular sieves)

Zeolites, also commonly referred to as molecular sieves, are hydrated alumino-silicates which are highly porous and are becoming more commonly used to capture molecules. The size of the pores can be adjusted by ion exchange and can be used to catalyze selective reactions (McCrady, 1996). The pores are also extremely uniform. Zeolites are especially effective at removing polar compounds, such as water and H_2S, from non-polar gas streams, such as methane (McKinsey Zicarai, 2003). Current research is focusing on how to implement zeolites in "clean coal" technology, or Integrated Gasification Combined Cycle (IGCC) power plants. Some studies about the use of zeolite-NaX and zeolite-KX as a catalyst for removing H_2S from IGCC gas streams have been performed at Yeungnam University in Korea. One study found a yield of 86% of elemental sulfur on the zeolites over a period of 40 hours (Lee, Jun, Park, Ryu, & Lee, 2005). Gas streams from IGCC power plants are at a high temperature, between 200 and 300°C. Further, molecular sieves have recently been used as a structural support for other types of adsorbents (Wang, Ma, Xu, Sun, & Song, 2005).

Polymers

There has not been significant research done using polymers as adsorbents for H_2S, but a a study was found where polymers were used in conjunction with other materials to enhance adsorption. This study, by Wang et al. (2008), studied the effects on H_2S adsorption of adding various compositions of a polymer, polyethylenimine (PEI), to a molecular sieve base. The mesoporous molecular sieves tested were amorphous silicates with uniform mesopores. PEI was deposited on the samples in varying compositions of 15-80 wt% of the molecular sieve. The results showed that the lower temperature tested (22°C) had higher sorption capacity, a loading of 50 wt% PEI on the molecular sieves had the best breakthrough capacity, and that a loading of 65 wt% PEI

www.manaraa.com

had the highest saturation capacity. Additionally, the sorbents can easily be regenerated for continued H_2S adsorption. The authors suggest that H_2S adsorbs onto the amine groups of the PEI, and at low compositions of PEI on the molecular sieves the amines present may be reacting with acidic functional groups on the molecular sieve surface. At high compositions of PEI on the molecular sieves, the surface area of the molecular sieve was significantly decreased and because the adsorption and diffusion rates of H_2S depend on surface area, the H_2S was not able to be effectively adsorbed.

Metal oxides

Metal oxides have been tested for hydrogen sulfide adsorption capacities. Iron oxide is often used for H_2S removal. It can remove H_2S by forming insoluble iron sulfides. The chemical reactions involved in this process are shown in the following equations:

$$Fe_2O_3 + 3H_2S \rightarrow Fe_2S_3 + 3H_2O \quad \text{(Eq. 12)}$$

$$Fe_2S_3 + 3/2O_2 \rightarrow Fe_2O_3 + 3S \quad \text{(Eq. 13)}$$

Iron oxide is often used in a form called “iron sponge” for adsorption processes. Iron sponge is iron oxide-impregnated wood chips. Iron oxides of the forms Fe_2O_3 and Fe_3O_4 are present in iron sponge. It can be regenerated after it is saturated, but it has been found that the activity is reduced by about one-third after each regeneration cycle (Abatzoglou & Boivin, 2009). Iron sponge can be used in either a batch system or a continuous system. In a continuous system, air is continuously added to the gas stream so that the iron sponge is regenerated simultaneously. In a batch mode operation, where the iron sponge is used until it is completely spent and then replaced, it has been found that the theoretical efficiency is approximately 85% (McKinsey Zicarai, 2003). Iron sponge has removal rates as high as 2,500 mg H_2S/g Fe_2O_3. Some challenges associated with the use of iron oxide for hydrogen sulfide removal from biogas are that the process is chemical-intensive, there are high operating costs, and a continuous waste stream is produced that must either be expensively regenerated or disposed of as a hazardous waste. There are some commercially produced iron oxide based systems that are able to produce non-hazardous waste. One commercially available iron oxide base system, Sulfatreat 410-HP® was found to have an adsorption capacity of 150 mg H_2S/g adsorbent through lab and field-scale experiments. (Abatzoglou & Boivin, 2009)

www.manaraa.com

The iron sponge is a widely used and long-standing technology for hydrogen sulfide removal. Because of this, there are accepted design parameters for establishing an H_2S removal system. Table 2 summarizes these design parameters.

Table 2, Iron sponge design parameter guidelines (McKinsey Zicarai, 2003)

Design Parameter	Guidelines
Vessels	Stainless-steel box or tower geometries are recommended for ease of handling and to prevent corrosion. Two vessels, arranged in series are suggested to ensure sufficient bed length and ease of handling.
Gas Flow	Down-flow of gas is recommended for maintaining bed moisture. Gas should flow through the most fouled bed first.
Gas Contact Time	A contact time of greater than 60 seconds, calculated using the empty bed volume and total gas flow, is recommended.
Temperature	Temperature should be maintained between 18°C and 46°C in order to enhance reaction kinetics without drying out the media.
Bed Height	A minimum 3 m bed height is recommended for optimum H_2S removal. A 6 m bed is suggested if mercaptans are present.
Superficial Gas Velocity	The optimum range for linear velocity is reported as 0.6 to 3 m/min.
Mass Loading	Surface contaminant loading should be maintained below 10 g S/min/m^2.
Moisture Content	In order to maintain activity, 40±15% moisture content is necessary.
pH	Addition of sodium carbonate can maintain pH between 8 and 10. Some sources suggest addition of 16 kg sodium carbonate/m^3 of sponge initially to ensure an alkaline environment.
Pressure	While not always practiced, 140 kPa is the minimum pressure recommended for consistent operation.

The iron sponge costs around $6/bushel (approx. 50 lbs) from a supplier, but other technologies that utilize iron sponge, such as the Model-235 from Varec Vapor Controls, Inc., can cost around $50,000 for the system and initial media (McKinsey Zicarai, 2003).

Other metal oxides besides iron oxide have been used to remove hydrogen sulfide. Carnes and Klabunde (2002) found that the reactivities of metal oxides depend on the surface area, crystallite size, and intrinsic crystallite reactivity. It was found that nanocrystalline structures have better reactivity with H_2S than microcrystalline structures, high surface areas promote higher adsorption, and high temperatures are ideal (but not higher than the sintering temperature, otherwise a loss of surface area occurs). Also, the presence of Fe_2O_3 on the surface furthers the reaction. The reason proposed for this was that H_2S reacts with the Fe_2O_3 to form iron sulfides that are mobile and able to seek out the more reactive sites on the core oxide and exchange ions, and ultimately acts as a catalyst in the reaction. However, at ambient temperatures this effect is not as

www.manaraa.com

clearly seen. In the study, calcium oxide was the most reactive (and with additions of surface Fe_2O_3 it was even more reactive), followed by zinc oxide, aluminum oxide, and magnesium oxide. In one study, Rodriguez and Maiti (2000) found that the ability of a metal oxide to adsorb H_2S depends on the electronic band gap energy: the lower the electronic band gap energy, the more H_2S is adsorbed. This is because the electronic band gap is negatively correlated to the chemical activity of an oxide and the chemical activity depends on how well the oxide's bands mix with the orbitals of H_2S. If the bands mix well, then the oxide has a larger reactivity towards the sulfur-containing molecules, and metal sulfides are created, which cause H_2S molecules to dissociate and the sulfur to be immobilized in the metal sulfides. Use of metal oxides for hydrogen sulfide removal can have problems such as low separation efficiency, low selectivity, high costs, and low sorption/desorption rate.

Zinc oxides are used to remove trace amounts of H_2S from gases at high temperatures (from 200°C to 400°C), because zinc oxides have increased selectivity for sulfides over iron oxides (McKinsey Zicarai, 2003). Davidson, Lawrie, and Sohail (1995) studied hydrogen sulfide removal on zinc oxide and found that the surface of zinc oxide reacts with the H_2S to form an insoluble layer of zinc sulfide, thereby removing H_2S from a gas stream. Approximately 40% of the H_2S present was converted over the ZnO adsorbent. The reaction described in Equation 14 leads to H_2S removal:

$$ZnO + H_2S \rightarrow ZnS + H_2O \qquad \text{(Eq. 14)}$$

Various commercial products use zinc oxide, and maximum sulfur loading on these products is typically in the range of 300 to 400 mg S/g sorbent (McKinsey Zicarai, 2003).

Sludge derived adsorbents

Because many commercially available adsorbents of H_2S are costly or have other associated problems, attention has been given to using various sludge derived materials as adsorbents. When sludge undergoes pyrolysis, a material is obtained with a mesoporous structure and an active surface area with chemistry that may promote the oxidation of hydrogen sulfide to elemental sulfur (Yuan & Bandosz, 2007). The mechanisms of H_2S removal described by Yan et al. (2004) can be applied to sludge derived adsorbents. Sludge has a complex chemistry, but it has enough of the reactive species given by Yan et al. that it could provide an alternative to using non-impregnated activated carbon. The efficiency of sludge at H_2S removal has been found to be similar to that of iron based adsorbents, but less efficient than impregnated activated carbon (Abatzoglou & Boivin, 2009).

www.manaraa.com

A concern with using sludge is that it may contain compounds which adversely affect H_2S removal. Some compounds in question are derived from metal sludge produced by industry. A study by Yuan and Bandosz (2007) mixed various weights of sewage sludge and metal sludge derived from a galvanizing process used in industry, pyrolyzed them, and tested them for hydrogen sulfide adsorption capacity. It was found that the capacity for H_2S adsorption is comparable to the capacity of impregnated activated carbons, and that the adsorption capacity depends on the overall sludge composition and the pyrolysis temperature. Samples with higher content of sewage sludge pyrolyzed at higher temperatures (800°C and 950°C) had the best adsorption capacity. The highest adsorption capacity reported was less than 21 mg H_2S/g adsorbent, which is less than the adsorption capacity of unimpregnated activated carbon.

Methods of Controlling Siloxane Emissions

Siloxanes must be removed from biogas before it is combusted in order to avoid silica particle formation. Some methods of siloxane removal are similar to hydrogen sulfide removal.

Chemical abatement

Chemical abatement is a reactive extraction process using contact between gas and liquids to facilitate the reactions. In chemical abatement, the Si-O bond in the siloxane molecule is broken. This reaction is catalyzed by strong acids such as HNO_3 and H_2SO_4. Alkalis can be used but there is the disadvantage that CO_2 is also retained, which increases the quantity of chemicals used and thus drives up the cost of treatment. (Abatzoglou & Boivin, 2009)

Adsorption

Activated carbon, molecular sieves, and silica gel have been investigated for use as an adsorbent for siloxanes. Adsorptive capacity has been found to depend on the type of siloxane present, where D5 has been found to adsorb better than other types of siloxanes. Silica gel can be an effective adsorbent, but the gas must be dried in order for maximum removal capacities to be achieved. The maximum removal capacity of silica gel has been found to be around 100 mg siloxane/g of silica gel. Silica gel can be regenerated, but the removal capacity decreases. Activated alumina and iron-based adsorbents have also been found effective at removing siloxanes. (Abatzoglou & Boivin, 2009)

www.manaraa.com

Absorption

Siloxanes are soluble in some organic solvents with high boiling points, such as tetradecane. These solvents can absorb siloxanes in spray or packed columns. Tetradecane has been found to have a 97% removal efficiency of D4 siloxane. However, this method is costly and is not economically feasible in small- to medium-scale facilities. (Abatzoglou & Boivin, 2009)

Cryogenic condensation

It has been found that freezing to temperatures of -70°C is necessary to remove more than 99% of siloxanes. At these low temperatures, siloxanes will condense and can be separated from the gas phase. It was found that at 5°C, 88% of siloxanes are still in the gas phase and at -25°C, 74% of siloxanes are still in the gas phase. Because of the extremely low temperatures needed for effective siloxane removal, this method is not feasible for small- to medium-scale facilities. (Abatzoglou & Boivin, 2009)

Particles Derived from Waste Rubber Products

This research utilizes waste rubber products, called tire derived rubber particles (TDRP) and other rubber materials (ORM). TDRP and ORM are produced and distributed by Envirotech Systems, Inc. The process by which TDRP is produced is proprietary, but information is available about other frequently used types of particles derived from used tires.

Particles from used tires

Approximately 281 million tires were discarded in the United States in 2001. This constitutes that, on average, there is one tire discarded every year for every person in the United States. There are applications that these tires, in various forms, can be used. Many of these applications require the tires be in a form called “crumb rubber”. Crumb rubber can generally be defined to be particle sizes of 3/8-inch or less. Crumb rubber can be classified into four groups:

1) Large or coarse (3/8”-1/4", or 9.525-6.350 mm),
2) Mid-range (10-30 mesh, 0.079”-0.039”, or 2.000-1.000 mm),
3) Fine (40-80 mesh, 0.016”-0.007”, or 0.406-0.178 mm), and
4) Superfine (100-200 mesh, 0.006”-0.003”, or 0.152-0.076 mm)

It is difficult to generalize particle size requirements in each market for crumb rubber, and therefore it is a challenge for crumb producers. However, rough estimates indicated that demand for the

www.manaraa.com

various sizes described are about 14% for coarse sizes, 52% for mid-range sizes, 22% for fine sizes, and 12% for superfine sizes. (Sunthonpagasit & Duffey, 2004)

Applications of rubber particles from used tires

Crumb rubber is used in various applications, and its use and demand has been increasing. Figure 1 shows the increase of crumb rubber utilization since 1994.

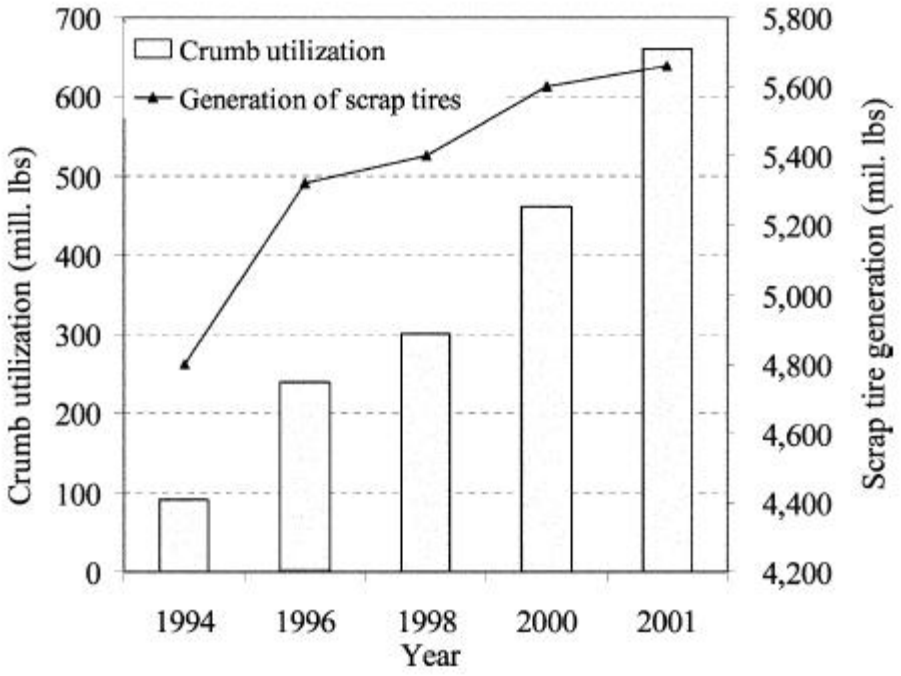

Figure 1, Scrap tire utilization (Sunthonpagasit & Duffey, 2004)

The largest application of used tires is tire derived fuel, where it is used as a supplemental fuel in cement kilns. This application accounts for approximately 33% of total scrap tires generated. Shredded rubber can be used in civil engineering applications, such as leachate collection in landfills and for highway embankments. These applications account for approximately 15% of scrap tires generated. Crumb rubber generation accounts for about 12% of scrap tires generated. Applications of crumb rubber include asphalt modification, molded products, sport surfacing, plastic blends, tires and automotive products, surface modification, animal bedding, and construction applications. Figure 2 describes the growing demand for crumb rubber in various applications from 1997 to 2001. (Sunthonpagasit & Duffey, 2004)

www.manaraa.com

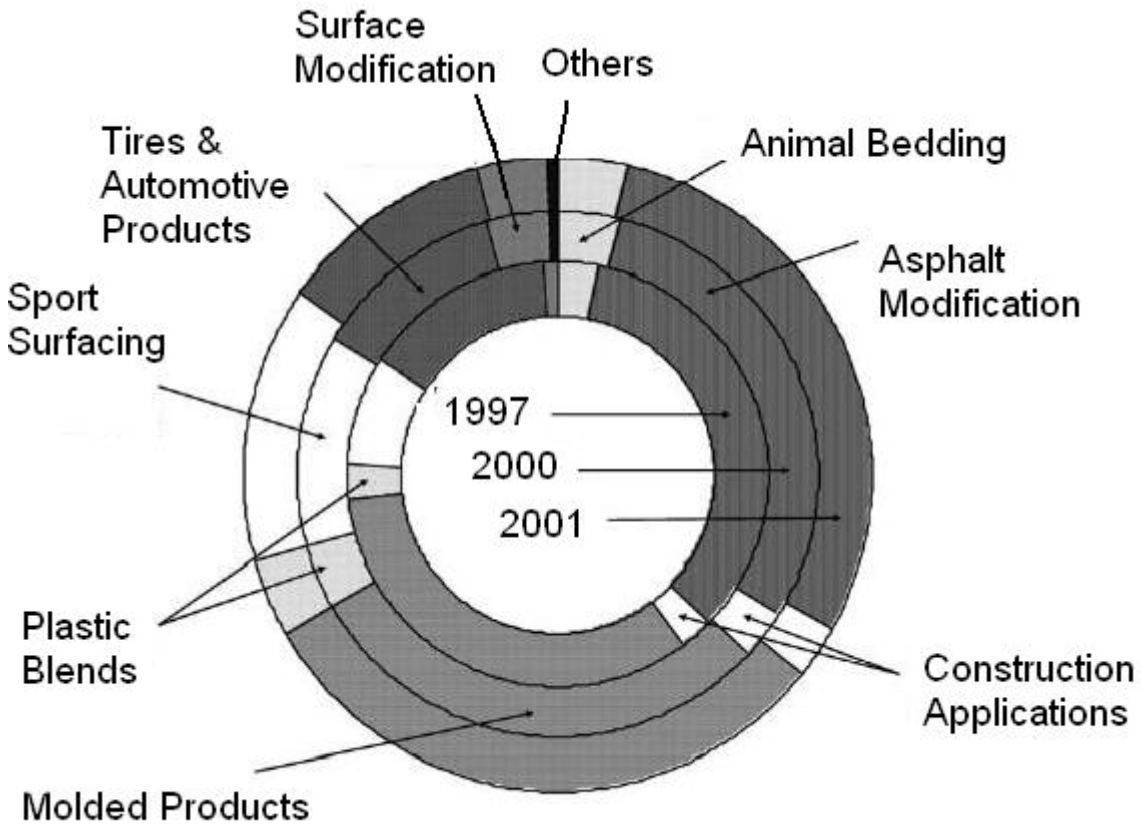

Figure 2, Crumb rubber markets (million pounds) in North America (Sunthonpagasit & Duffey, 2004)

There are few standards for quality and production in the crumb rubber industry. Sunthonpagasit and Duffey (2004) found that definitions of quality appear to be diverse and driven by customer specifications unique to different market segments, but in general, high quality means low fiber content (less than 0.5% of total weight), low metal content (less than 0.1% of total weight), high consistency, and a moisture content of about 1% by weight. The moisture content limit is because applications such as molding and extruding have specific heat requirements that would not be met if excess moisture needed to be removed from the rubber.

Environmental risks of using scrap tire materials

The most cited concerns of using scrap tire materials relate to water quality. It has been found that as long as the tire shreds are placed above the water table, they appear to pose no significant risk to either health or the environment. The constituents of tire rubber do not increase the concentration of metals of concern in meeting primary drinking water standards. However, steel

www.manaraa.com

belts are exposed at the cut edges of the tire shreds, which may increase the levels of iron and manganese, affecting secondary drinking water standards. (Sunthonpagasit & Duffey, 2004.)

There may also be issues with worker exposure to fine respirable particles and particle-bound polycyclic aromatic hydrocarbons (PAHs). One study of road paving workers using crumb rubber modified asphalt found potential exposure to "elevated airborne concentrations of a group of unknown compounds that likely consist of the carcinogenic PAHs benz(*a*)anthracene, chrysene and methylated derivatives of both." (Sunthonpagasit & Duffey, 2004)

Crumb rubber production

The process of crumb rubber production can vary with end-use applications. However, Sunthonpagasit and Duffey (2004) generalize the process of producing 3/8" (9.525 mm) to 80 mesh (0.178 mm) crumb rubber particles in Figure 3:

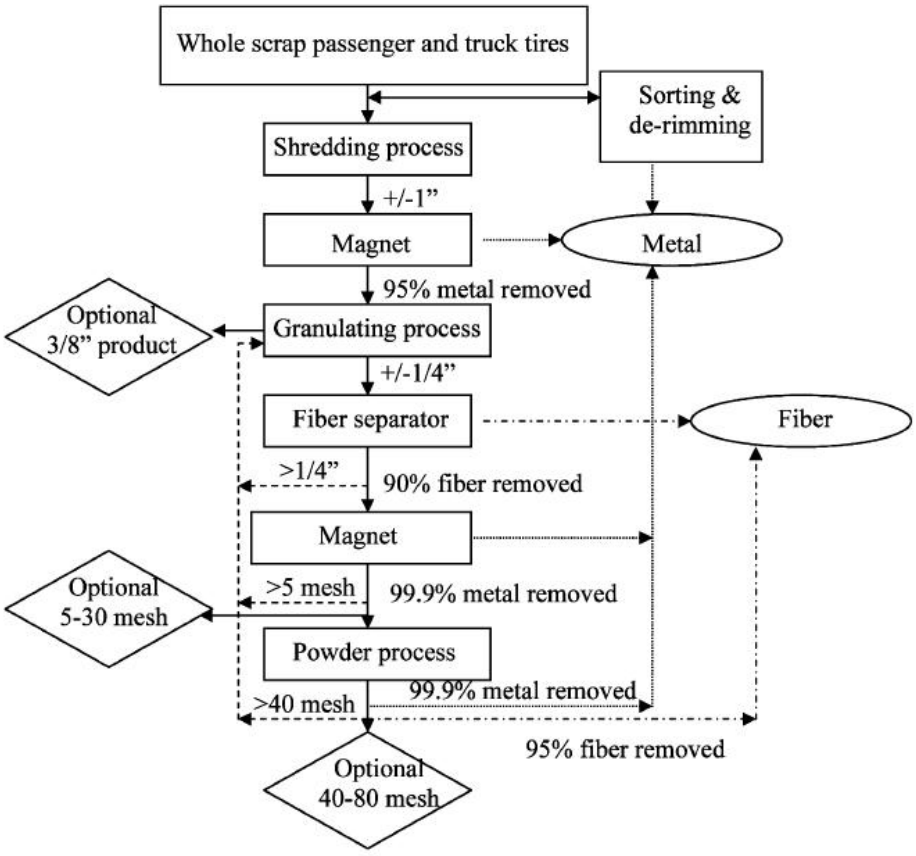

Figure 3, Generalized crumb rubber production (Sunthonpagasit & Duffey, 2004)

www.manaraa.com

Crumb production processes occur at ambient temperatures in the majority of production operations. Most operations separate passenger car and truck tire processing. In the production process, after tires are first separated into truck and passenger car tires, the tires are de-rimmed and shredded and/or granulated to a mesh size of approximately 3/8" (9.525 mm) or 5-30 mesh. The 3/8" (9.525 mm) product has about 5% metal and the 5-30 mesh product has about 0.1% metal. These products can either be sold as-is or reduced to smaller sizes, depending on the application. After granulation, the process to produce smaller mesh sizes is referred to as the "powder process". The amount of rubber waste following each process is 8% for shredding, 6% for granulating, and 4% for the powder process. (Sunthonpagasit & Duffey, 2004)

Other production considerations include the type of processing equipment that is needed and the condition of the processing equipment. As truck tires usually have large amounts of reinforcing wires in them, they are more difficult to process and therefore require different processing equipment than that needed for passenger car tires. The condition of the processing equipment also plays a significant role in the quality of the product and in the maintenance costs associated with processing. (Sunthonpagasit & Duffey, 2004)

Tire characteristics

On average a passenger car tire is equivalent to about 20 lbs. Each passenger car tire contains approximately 86.0% rubber compound, 4% fiber, and 10% metal. Truck tires are about 100 lbs and contain approximately 84.5% rubber compound, less than 0.5% fiber, and 15 % metal. The composition of the processed tires will change somewhat, due to processing techniques such as magnetic metal removal, which also removes rubber particles that are attached to the ferrous metals. (Sunthonpagasit & Duffey, 2004)

Tires are made of vulcanized rubber and other reinforcing materials. Vulcanized rubber is a polymer with cross-linked chains. The reinforcing materials include fillers and fibers. Fillers are generally made of carbon black, which strengthens the rubber and provides abrasion resistance. Fibers are made of textiles or steels, usually in the form of a cord, which provide strength and a tensile component. The rubber compound in the tires is generally of the composition listed in Table 3.

www.manaraa.com

Table 3, Rubber compound composition (Amari et al., 1999)

Component	Mass %
Styrene-butadiene	62.1
Carbon black	31.0
Extender oil	1.9
Zinc oxide	1.9
Stearic acid	1.2
Sulfur	1.1
Accelerator	0.7
Total	99.9

Organo-sulfur compounds, zinc oxide, and stearic acid are used as vulcanizing agents. Styrene-butadiene (SBR) is a co-polymer most commonly used as the rubber matrix. Sometimes it is a blend of natural rubber and SBR. Extender oil is usually petroleum oil which is used to control viscosity, reduce internal friction during processing, and improve low temperature flexibility in the vulcanized product. The accelerator aids in vulcanization. (Amari, Themelis, & Wernick, 1999)

Characteristics of TDRP and ORM

The TDRP and ORM were previously characterized in a past study (Ellis, 2005) using sieve analyses and a chemical analysis. Figure 4 and Figure 5 show sieve analyses of ORM and TDRP performed as part of this study. These sieve analyses show that ORM has a well balanced spread of particle sizes over a larger range of sizes. On the other hand, TDRP has more of the material over a smaller range of sizes.

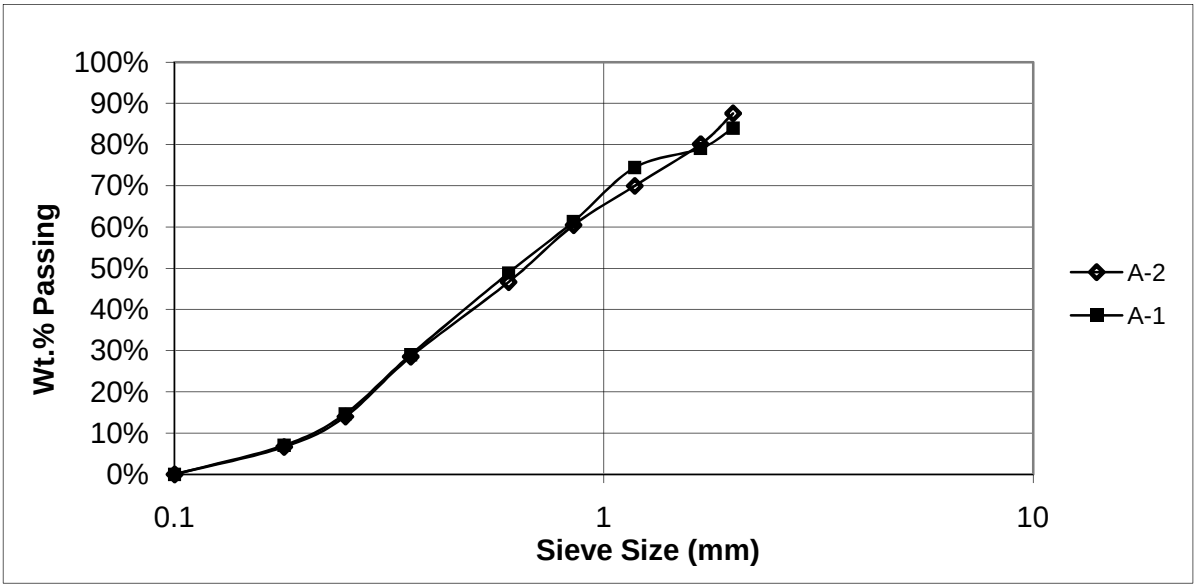

Figure 4, Sieve analysis of ORM for 2 samples (Ellis, 2005)

www.manaraa.com

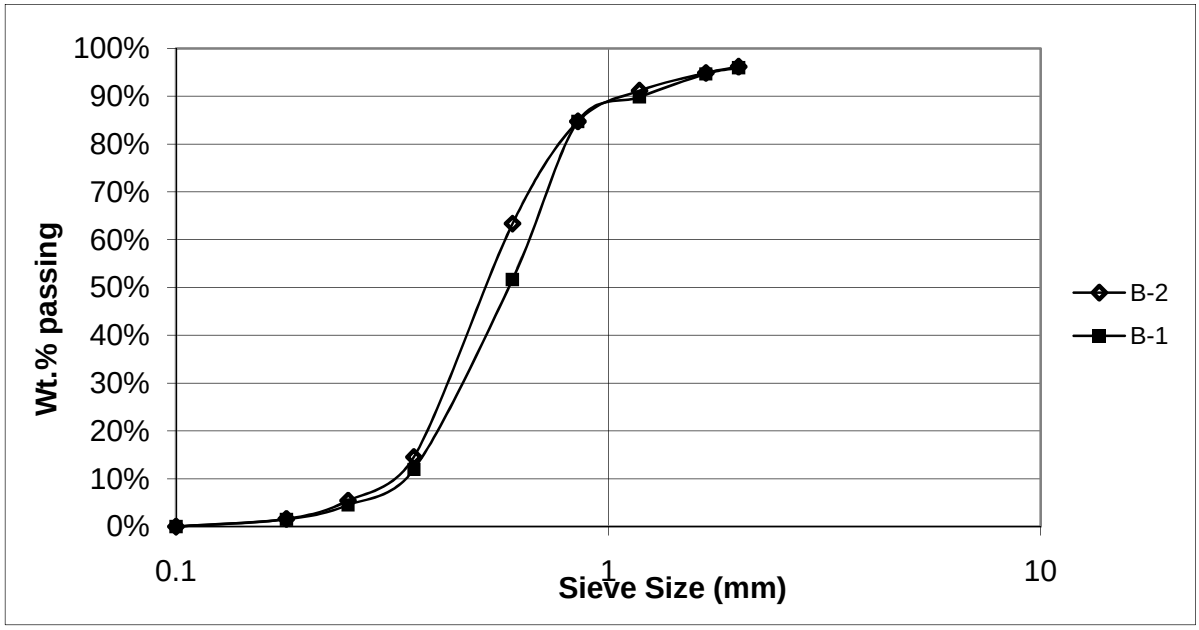

Figure 5, Sieve analysis of TDRP for 2 samples (Ellis, 2005)

A chemical analysis performed in the same study found that TDRP and ORM contained zinc, magnesium, chlorine, sulfur, silicon, calcium, and oxygen. Information was not available about concentrations and specific differences between TDRP and ORM. Information provided by Envirotech Systems, Inc. said that TDRP had "metal additions" and ORM did not, but no specific information was available. TDRP is shown in Figure 6.

Figure 6, TDRP at a magnification of 1.5X

www.manaraa.com

Experimental Methods

Because tire particles have not been used in H_2S removal applications, there is no existing literature about experimental methods. Experimental methods for H_2S removal from literature were referred to as a basis for creating an experimental method and apparatus for testing the tire particles.

ASTM: D 6646-03. Standard Test Method for Determination of the Accelerated Hydrogen Sulfide Breakthrough Capacity of Granular and Pelletized Activated Carbon

The American Society for Testing and Materials, ASTM International, provides a standard regarding the testing of the breakthrough capacity of GAC. This method is for virgin, newly impregnated or in-service, granular or pelletized activated carbon with a mean particle diameter less than 2.5 mm meant to remove hydrogen sulfide from an air stream. Although this standard provides accepted methodology for activated carbon, it is not necessarily applicable to non-carbon adsorptive materials.

This method defines breakthrough of the activated carbon to be when the outlet gas stream of an activated carbon bed has a concentration of 50 ppmv H_2S when the inlet concentration is 10,000 ppmv H_2S. It is emphasized that this test does not simulate actual conditions encountered in real-life situations and is only meant to compare the breakthrough of different carbons. One of the reasons is that the column size, 23 cm, has a mass transfer zone that is proportionally much larger than the typical bed used in practical application and causes carbons with rapid kinetics for H_2S removal to be favored over carbons with slower kinetics.

The recommended gas used in this method is nitrogen with controlled H_2S concentrations. The H_2S sensor should be able to reliably detect 50 ppm, and either “solid state” or electrochemical type sensors are suggested. The media bed is located in an adsorption tube, which has specific dimensions as shown in Figure 7.

www.manaraa.com

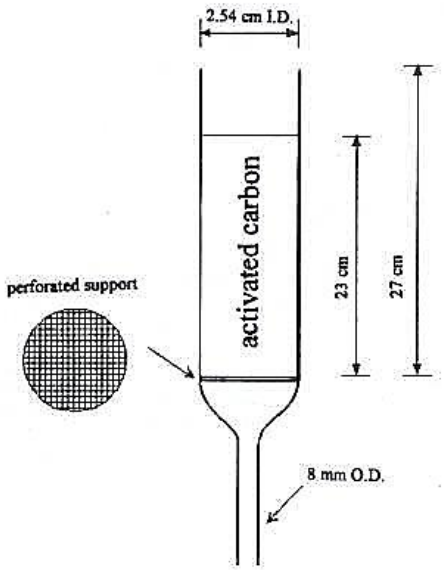

Figure 7, Schematic of adsorption tube (ASTM, 2003)

A way of controlling the flow of gas is needed. It is recommended that a flow meter, mass flow controller, or rotameter with corrosion resistant parts be used with the potential of measuring flow rates of 0-2,000 mL/min nitrogen. A source of dry, contaminant-free air capable of delivering up to 2 L/min is needed to mix with the H_2S to the desired concentration, 10,000 ppm (1 vol%) H_2S. Also needed are: an air line pressure regulator to maintain up to 10 psig pressure for up to 2 L of air/min, two metering valves, a gas bubbler to ensure the generation of a 80% relative humidity air stream, H_2S calibration gas, and a timer. The entire schematic should be similar to Figure 8.

www.manaraa.com

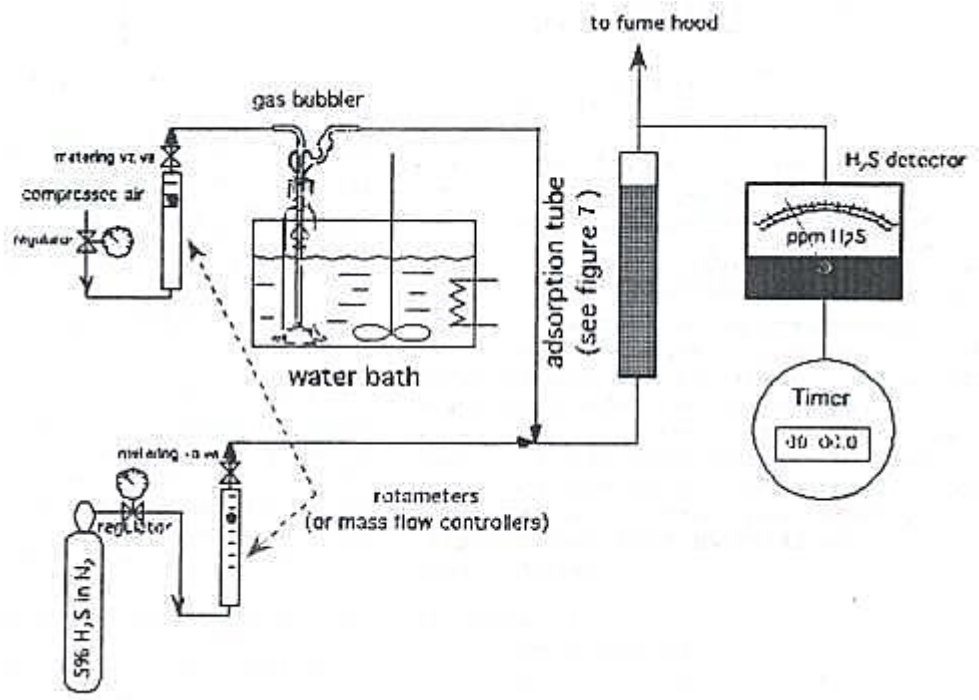

Figure 8, Schematic of apparatus for determination of H_2S breakthrough capacity (ASTM, 2003)

To run the system, the H_2S/N_2 system should first be adjusted to produce a 10,000 ppm H_2S stream at a total flow rate of 1,450 cm^3/min. For the media bed, 116 mL of carbon should be used. It should be placed in the bed using a vibratory feeder. The system should be run until an outlet concentration of 50 ppmv H_2S is reached. (ASTM, 2003)

The main calculation derived from this test is the H_2S breakthrough capacity of the GAC in g H_2S/cm^3 GAC. The calculation is as follows, assuming standard conditions:

$$\frac{g\ H_2S}{cm^3\,GAC} = \frac{\left(\frac{C}{100}\right) \times F \times T \times \left(\frac{1\ L}{1000\ cm^3}\right) \times \left(\frac{1\ mole}{22.4\ L}\right) \times \left(\frac{34.1\ g\ H_2S}{mole}\right)}{V} \qquad \text{(Eq. 15)}$$

where: C = concentration of H_2S in air stream, volume %

F = total H_2S/air flow rate, cm^3/min

T = time to 50 ppmv breakthrough, min and

V= actual volume of the carbon bed in the absorption tube, cm^3

The apparent density of the GAC can then be used to convert this into units of g H_2S/g GAC. According to the standard the sample average and standard deviation are calculated, and if the

www.manaraa.com

standard deviation is within 10% of the average, it can be reported as the H_2S breakthrough capacity. (ASTM, 2003)

This system is the closest standard that exists for H_2S removal in an adsorptive bed. This experimental method is very strictly controlled and is meant to be used in a laboratory environment.

Other experimental systems

The literature available about H_2S removal onto an adsorbent describes various laboratory-controlled experiments with various experimental parameters. A few of these experiments are reviewed here.

The relative humidity is usually 70% or 80%. The temperature of the gas is held around 25°C or slightly higher. Inlet concentrations of H_2S are usually varied throughout the course of the experiment to establish isotherms, and are usually incremented between 1,000 ppmv and 5,000 ppmv. The dimensions of the reaction column differ slightly between studies, but are generally about 200-400 mm in length, either 8-9 mm or much larger, such as 2.5 cm-6.5 cm in diameter, and 15 to 23 cm in bed height. These dimensions are often structured around the ASTM standard, depending on the adsorbent being used. Flow rates are from 0.12 L/min to 0.5 L/min. The temperature inside the column is controlled, and a temperature of about 25°C is often used, but sometimes elevated temperatures, such as 60°C are used. The contact time in the scrubber depends on both the volume of the media bed and the flow rate, but was found to be either very small, on the order of 0.5 s, or much higher, such as 30 or 60 seconds. The experiments are generally stopped when a certain concentration of H_2S is detected in the outlet gas. These concentrations are from 10 ppm to 500 ppm. (Bandosz, 2002; Bagreev et al., 2005; Xiao, Wang, Wu, & Yuan, 2008; Truong & Abatzoglou, 2005; and Yuan & Bandosz, 2007)

Of course, these parameters are varied depending on the scope of the experiment, and it is difficult to generalize a H_2S adsorption experiment.

www.manaraa.com

CHAPTER 3. THEORY

Adsorption

Adsorption is a process used to remove undesirable compounds in gas or liquid streams by passing the stream through a media bed composed of a solid material. The solid material used is called the adsorbent and the gas or liquid compound being adsorbed is called the adsorbate. In adsorption, the adsorbate penetrates into the pores of the adsorbent, but not into the lattice itself (Davis & Cornwell, 2008). Only gas streams were used in this research project and therefore this review will henceforth only apply to gas streams. The adsorption process can be used to dehumidify gas, remove odors or pollutants from the stream, or recover valuable solvent vapors from the stream. Adsorption has been found to be particularly applicable to gas that is noncombustible or difficult to burn, pollutants that are valuable when recovered, and pollutants that are in very dilute concentrations (Wark, Warner, & Davis, 1998).

The mechanisms of adsorption are either physical or chemical. In physical adsorption, intermolecular forces cause the gas molecules to be attracted to and adhere to the surface of the adsorbent. The adsorption process is always exothermic, and the amount of heat released depends on the magnitude of the attractive force but is usually between 2 and 20 kJ/g·mol. Physical adsorption is usually reversible by either lowering the pressure of the adsorbate in the gas stream or raising the temperature, which makes regenerating and reusing the spent adsorbent possible. Because physical adsorption involves the adherence of gas molecules to the surface of the adsorbent, the adsorption capacity is directly proportional to the surface area of the adsorbent. However, the adsorbent is not limited to a single layer of molecules on the surface; multiple layers of adsorbate molecules may accumulate. In chemical adsorption, or chemisorption, a chemical reaction occurs between the adsorbate and the adsorbent. The chemical reactions that occur in chemisorption have much stronger bonds than the physical attractive forces in physical adsorption, on the range of 20 to 400 kJ/g·mol. Chemisorption is usually not reversible and only a single layer of adsorbate molecules may be present on the surface because the valence force adhering the adsorbate to the adsorbent are only effective over extremely short distances. (Wark et al., 1998)

A material used as an adsorbent must have certain properties in order to be an effective adsorbent. Particle diameters can range from about 1.3 cm to less than 200 µm and the material

www.manaraa.com

should have a high surface area per unit weight ratio. Some materials that are effective adsorbents have extremely high surface area per unit weight ratios due to the surface area of internal pores on the solid. If the pore diameter is a few times larger than the molecular diameter of the adsorbate, the pores will be readily available for adsorption. Another advantageous property of the adsorbent is if it has a chemical affinity for the adsorbate. Materials commonly used for adsorption were discussed in depth in the Literature Review. (Wark et al., 1998)

An adsorption system should be designed with respect to the properties of both the adsorbent and the adsorbate. Some requirements for an adsorption system identified by Wark et al. are the provision for sufficient dwell time, the pretreatment of the gas stream to remove non-adsorbable matter and remove high concentrations of competing gases, good distribution of flow through the bed, and a provision of regenerating the adsorbent bed after saturation. Sufficient dwell time (contact time) is necessary so that the physical and/or chemical reactions have time to occur. It is necessary to remove non-adsorbable matter because it may impair the operation of the adsorbent bed. Similarly, it is important to remove high concentrations of competing gases so that the system does not get overburdened and become ineffective at removing the pollutant of concern. Operation of a system can be in either a batch or continuous mode and may involve a regenerative process. Generally, if the pollutant is on the order of 1 to 2 ppm or less, the adsorbent is discarded rather than regenerated. However, this is also dependent on the nature of the pollutant and whether it is highly volatile once adsorbed. If continuous operation is used, it is common to have two beds in parallel so that one can be regenerating (or being replaced) while the other is being used for adsorption. (Wark et al., 1998)

Adsorption isotherms are useful tools for modeling adsorption behavior. An adsorption isotherm relates the volume or mass adsorbed to the partial pressure or concentration of the adsorbate in the gas stream at a constant temperature. Experimental adsorption data has shown that increasing the pressure of the adsorbate in the gas stream causes a higher amount to be adsorbed. Increases in temperature of adsorption systems have been found to decrease the amount adsorbed, and therefore it is usually desirable to operate an adsorption system at as low a temperature as possible. Additionally, it has been found that adsorption improves with an increase in the molar mass of the adsorbate. (Wark et al., 1998)

www.manaraa.com

Various theories have been developed to describe experimental adsorption behavior. The most common theoretical models are the Langmuir Isotherm, the Brunauer-Emmett-Teller (B.E.T.) Model, and the Freundlich Isotherm. The Langmuir Isotherm assumes that adsorption occurs on a fixed number of sites that are all energetically equivalent, each site can adsorb only one molecule, and interactions between adsorbed molecules are neglected because they are assumed to be small compared to the interaction between the adsorbate and the adsorbent (Keller & Staudt, 2005). The Langmuir isotherm is described in Eq. 16,

$$\frac{C_g^*}{W} = \frac{1}{a} + \frac{b}{a} C_g^* \qquad \text{(Eq. 16)}$$

where W is the amount of gas per unit mass of adsorbent (kg/kg), C_g^* is the equilibrium concentration of gaseous pollutant (g/m^3), and *a* and *b* are constants which are experimentally determined (Davis & Cornwell, 2008). The Langmuir model was chosen as one of the isotherms to model the experimental data.

The B.E.T. Model is an extension of the Langmuir Isotherm and it describes multiple layers of molecules that are adsorbed on the surface of an adsorbent. The B.E.T. equation (Eq. 17), which is associated with this model, is based on the rates of condensation and evaporation from the layers of molecules on the surface of the adsorbent:

$$\frac{V}{V_m} = \frac{cP}{(P_0 - P)[1 + (c-1)\left(\frac{P}{P_0}\right)]} \qquad \text{(Eq. 17)}$$

where V is the volume of adsorbed gas would fill at a given temperature and pressure, V_m is the volume adsorbed if a layer one molecule thick fills the surface, P_0 is the vapor pressure of the adsorbate at the system temperature, P is the actual partial pressure of the adsorbate in the gas stream, and *c* is a parameter associated with the adsorption process. V_m and *c* are determined experimentally. Research has found that the B.E.T. equation may be difficult to evaluate if values of P/P_0 are less than 0.05 or greater than 0.35. (Wark et al., 1998)

The Freundlich Isotherm is another type of isotherm used to describe the adsorption of a single layer of molecules onto an adsorbent. It is commonly used to fit experimental data. It is described in Eq. 18:

www.manaraa.com

$$C_e = \alpha X_{sat}^{\beta} \qquad \text{(Eq. 18)}$$

where C_e is the equilibrium concentration of the pollutant with the adsorbent, X_{sat} is the saturated adsorbent concentration, and α and β are experimentally determined constants. The Freundlich isotherm was also used to model data in this research because of its simplicity and ability to successfully model experimental data. (Wark et al., 1998)

As the pollutant moves through the media bed, some is adsorbed onto the adsorbent located closest to the inlet gas. When that part of the adsorbent bed becomes saturated with the adsorbate, it cannot adsorb any more of the adsorbate and the adsorption process continues with the adsorbent located next to it. This continues down the length of the media bed. In this manner, the adsorption of the adsorbate onto the adsorbent can be said to occur in a "wave", as shown in Figure 9.

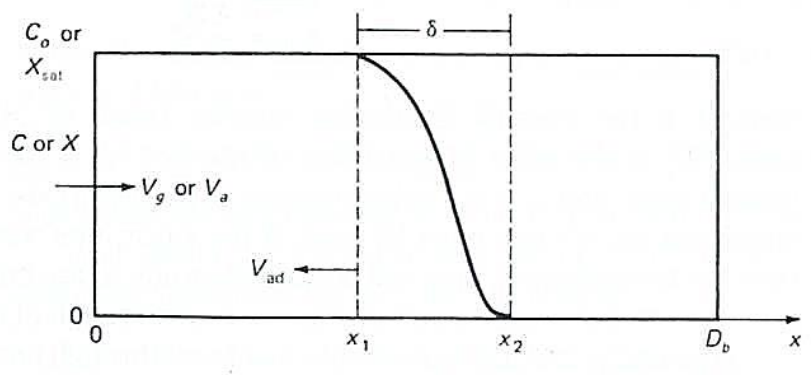

Figure 9, Adsorption wave (Wark, Warner, & Davis, 1998)

Figure 9 shows the velocity of the adsorption wave, V_{ad}, through the bed of depth D_b. At point x_1 along the length of the bed, the bed up until x_1 is completely saturated with adsorbate (concentration of adsorbate on the adsorbent is X_{sat} and concentration of adsorbate in the main gas stream is the inlet concentration, C_0). At point x_2, which is farther from the inlet gas than x_1, the bed does not have any adsorbate adsorbed on it (concentration, C, is zero). The difference in length from points x_1 to x_2 is δ, which is known as the width of the adsorption zone, and is where the active adsorption processes are occurring. When point x_2 reaches point D_b, the concentration of the pollutant in the outlet gas will begin to increase and "breakthrough" will occur in the bed. When

www.manaraa.com

point x_1 reaches D_b the adsorbent bed will be completely saturated with the adsorbate and the outlet pollutant concentration will be the same as the inlet pollution concentration.

Assuming behavior consistent with the Freundlich Isotherm and using a mass balance on the pollutant in the adsorption zone, an equation can be derived describing the velocity of the adsorption wave as

$$V_{ad} = \frac{\dot{m}_a}{\rho_a \rho_{ad} A} \alpha^{1/\beta} C_o{}^{(\beta-1)/\beta} \qquad \text{(Eq. 19)}$$

where $\dot{m}_a$ is the mass flow rate of the carrier gas, ρ_a is the density of the carrier gas, ρ_{ad} is the apparent bulk density of the adsorbent, A is the area of the bed cross-section, C_0 is the inlet concentration of H_2S, and α and β are constants, as described in Eq. 18 (Wark et al., 1998). Because this equation is based on an isotherm, the α and β constants are temperature dependent. For the current adsorption system, the carrier gas is the biogas, the adsorbent is the TDRP, and the inlet concentration C_0 can be assumed to be equivalent to the equilibrium concentration, C_e, described in Eq. 18.

To find the width of the adsorption zone, δ, further relationships between concentration and distance in the media bed (x) can be derived. Wark et al. (1998) describes in detail the process of deriving these relationships. Equation 20 shows the relationship of δ to concentration as a result of some of these derivations. In Eq. 20, η represents the ratio of concentration to inlet concentration of the adsorbate in the main gas stream (C/C_0):

$$\frac{\delta K A \rho_a}{\dot{m}_a} = \int_0^1 \frac{d\eta}{\eta(1-\eta^{\beta-1})} \qquad \text{(Eq. 20)}$$

where K is a film coefficient for the transfer process that takes into account the film resistance as well as the effective interfacial area of the adsorbent. The integral in Eq. 5 is undefined at the boundaries of η=0 and η=1, but using values close to these boundaries will allow the integral to be evaluated. Wark et al. uses boundaries of η=0.01 to η=0.99, which is the same as defining an adsorption zone width such that C approaches within 1% of its limiting values of 0 and C_0. Evaluating the integral at these boundaries, substituting equivalent terms, and defining the adsorption zone width to be x_2-x_1 gives Eq. 21, which describes the shape of the concentration versus distance curve:

www.manaraa.com

$$x = x_1 + \frac{\dot{m}_a}{KA\rho_a}\left[ln\frac{0.99C_0}{C} + \frac{1}{\beta - 1}ln\frac{1-(\frac{C}{C_0})^{\beta-1}}{1-(0.99)^{\beta-1}}\right] \quad \text{(Eq. 21)}$$

Different values of η can be chosen, depending on the acceptable limit of pollutant in the outlet gas (there are different definitions of when breakthrough occurs).

The time of breakthrough can be predicted using Eq. 22 if δ is known and if it is assumed that the time required to establish the full width of the adsorption zone at the inlet is zero:

$$t_B = \frac{D_b - \delta}{V_{ad}} \quad \text{(Eq. 22)}$$

Combining Eq. 19 and 22 gives an expression for the volume of media needed:

$$A(D_b - \delta) = \frac{\dot{m}_a t_B}{\rho_a \rho_{ad}} \alpha^{1/\beta} C_o^{(\beta-1)/\beta} \quad \text{(Eq. 23)}$$

Application of Theory to Experimental Data

As previously mentioned, the Freundlich isotherm (Eq. 18) was used to model the experimental data in this study. The use of Eq. 18 requires values for C_e, the equilibrium concentration of the adsorbate with the adsorbent, and X_{sat}, the saturated adsorbent concentration. The equilibrium concentration, C_e, was assumed to be the inlet adsorbate concentration because this study used a continuous adsorption system instead of a batch system. The inlet adsorbate concentration was found experimentally by averaging the inlet pollutant concentration before breakthrough occurred. The saturated adsorbent concentration was assumed to be the amount of adsorbate removed from the inlet gas up until the time of breakthrough. Figure 10 shows an example of a breakthrough curve from this study. Every hour, a sample of both the inlet and outlet gases from the system was taken. The amount of adsorbate (H_2S in this study) removed from the inlet gas up until the time of breakthrough was determined with this experimental data by converting the H_2S concentration to mg of H_2S per gram of TDRP (the adsorbent), then integrating the area between the inlet and outlet curves.

www.manaraa.com

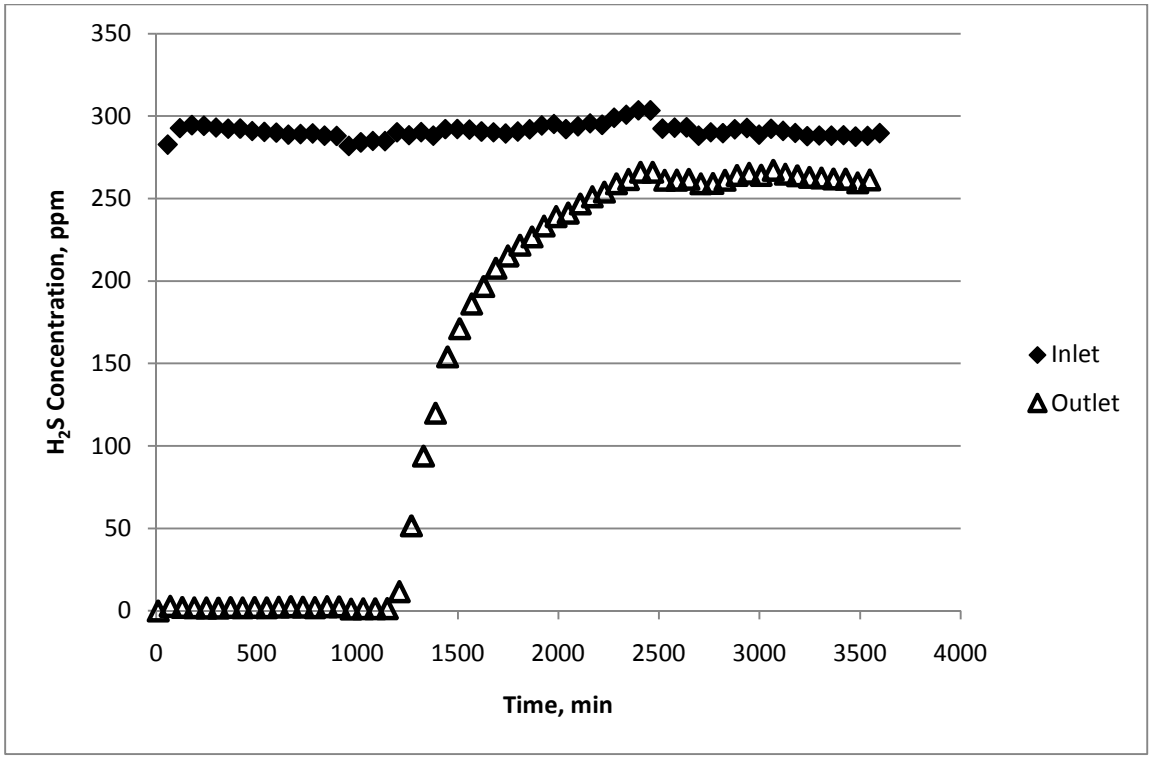

Figure 10, Example of a breakthrough curve from the study

Integration of the curves was performed using the trapezoid method. The trapezoid method approximates the area under a curve by averaging the height of 2 consecutive points on the curve and multiplying it by the horizontal distance between the 2 points. This is shown graphically in Figure 11.

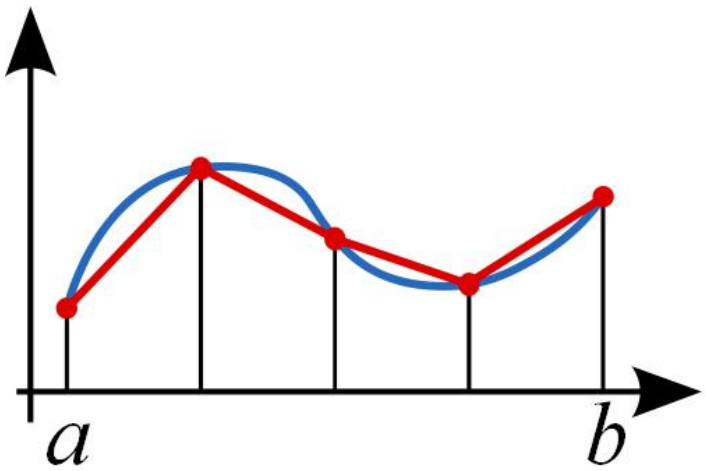

Figure 11, Graphical representation of the trapezoid method for integrating a curve (Trapezoidal Rule, 2010)

www.manaraa.com

In the case of Figure 10, both the inlet curve and the outlet curve were integrated up until the point of breakthrough using the trapezoid method, then the value obtained for the outlet curve was subtracted from the value obtained for the inlet curve. This area between the inlet and outlet curves represents the amount of H_2S removed from the inlet stream by the TDRP, and is therefore a close approximation of the value of X_{sat}.

Equation 18 can be manipulated to yield Eq. 24:

$$\log(C_e) = \log(\alpha) + \beta \log(X_{sat}) \quad \text{(Eq. 24)}$$

Experimental data was used for C_e and X_{sat}. A linear trendline was fit to the resulting plot. From this trendline, α and β were determined (α was found by equating log(α) to the y-intercept of the linear line and β was the slope of the line). Once α and β were determined, they were applied to Eq. 23. As noted, Eq. 23 gives an expression for the volume of media needed using the media bed length D_b, the width of the adsorption zone δ, and the area A. Because δ is difficult to determine from experimental data due to its relatively small value, δ was assumed to be zero for the purpose of practical calculations. By assuming δ to be zero, the calculated length of the media bed, D_b, is the length of the bed needed for complete saturation to occur. By applying a safety factor (SF) to the volume of calculated media needed, sudden (and possibly catastrophic) breakthrough is avoided. Applying this to Eq. 23 gives Eq. 25.

$$Volume = SF \cdot AD_b = SF \cdot \frac{\dot{m}_a t_B}{\rho_a \rho_{ad}} \alpha^{1/\beta} C_o{}^{(\beta-1)/\beta} \quad \text{(Eq. 25)}$$

This theory lays the groundwork for the calculations that follow in the Results section.

www.manaraa.com

CHAPTER 4. MATERIALS AND METHODS

Experimental Apparatus

Gas flow through system

The experimental apparatus was set-up and maintained at the WPCF in the Gas Handling Building. A schematic of the scrubber system is shown in Figure 12.

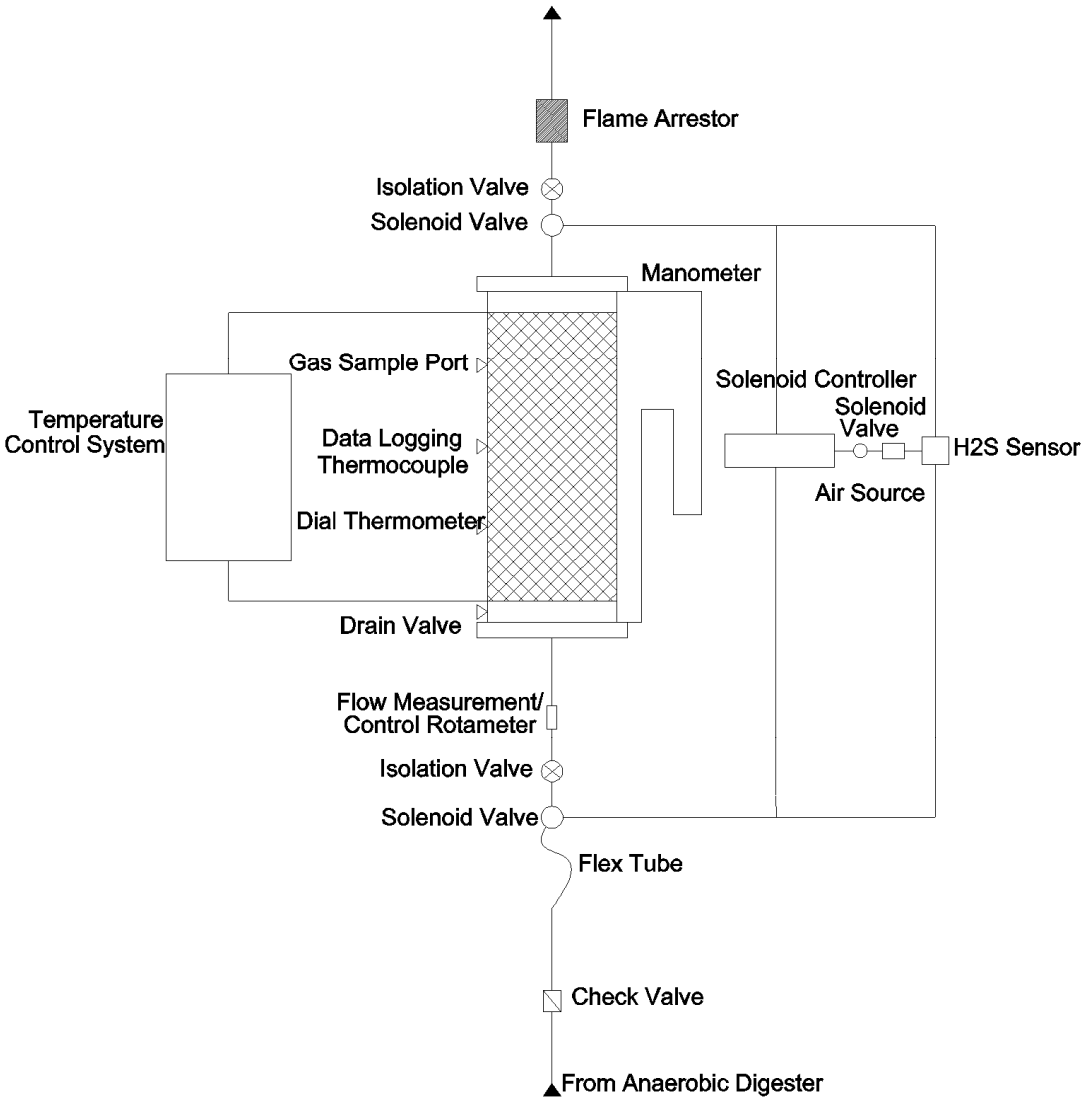

Figure 12, Schematic of scrubber system

www.manaraa.com

As shown in Figure 12, the biogas from the anaerobic digesters at the WPCF entered the system and first passed through a check valve to prevent any backflow from entering the gas handling system. The gas was then either sampled by the H_2S detector if the solenoid controller opened the solenoid valve, or continued to pass through an isolation valve and rotameter and into the scrubber. The isolation valve was used to shut off gas flow to the system if necessary and the rotameter was used to control the flow through the system. The scrubber was temperature controlled by the temperature control system. The temperature control system pumped water through copper tubes that were wound around the outside of the scrubber and then insulated. Once the gas entered the scrubber, it passed through the media bed. The pressure difference in the scrubber could be read from manometers located both at the inlet and outlet sides of the scrubber. Two different thermometers were located in the scrubber. One was a data logging thermocouple, which recorded a temperature reading every 30 seconds. The other was a dial thermometer, which was used to corroborate the readings from the thermocouple and also when the data logging thermometer was not properly functioning. There was also a gas sample port located on the scrubber and a drainage valve underneath it to remove condensation.

After the gas passed through the media bed, it flowed out of the scrubber and then could be sampled by the H_2S detector through the solenoid valve. It then passed through another isolation valve and a flame arrestor as safety precautions. The outlet gas was exhausted outside the Gas Handling Building.

An air source was also attached to the H_2S detector. This was controlled by the solenoid controller, and it was run in between inlet and outlet gas sampling times in order to stabilize the detector. The gas being sampled or run through the H_2S detector also was exhausted outside the Gas Handling Building.

The actual set-up of the scrubber system is shown in Figure 13. Figure 13 depicts the acrylic scrubber housing and all related appurtenances and controls. The system was designed to split the flow of the biogas into two scrubbers so that simultaneous experiments could be run. However, the flow of biogas through the system was not enough to divide between two scrubbers and only one of the scrubbers was utilized in this study (the scrubber seen on the left).

www.manaraa.com

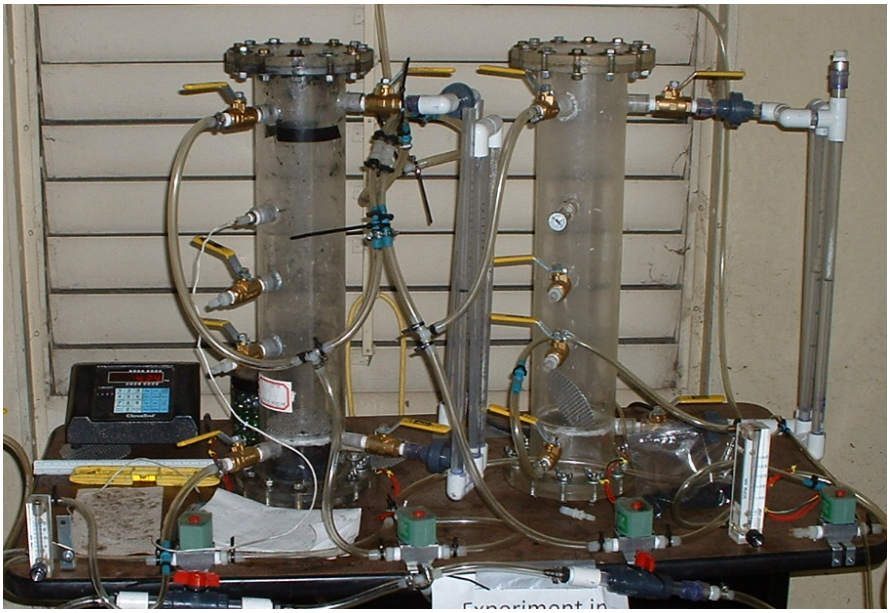

Figure 13, Scrubber system

Figure 14 shows the system with the addition of the temperature control system. The scrubber that was utilized for experiments was insulated after copper tubing carrying temperature controlled water was wrapped around it. Parts of the system are labeled in Figure 14, as shown in the schematic in Figure 12. For scale, the rotameter on the left side of the table is 10.2 cm tall.

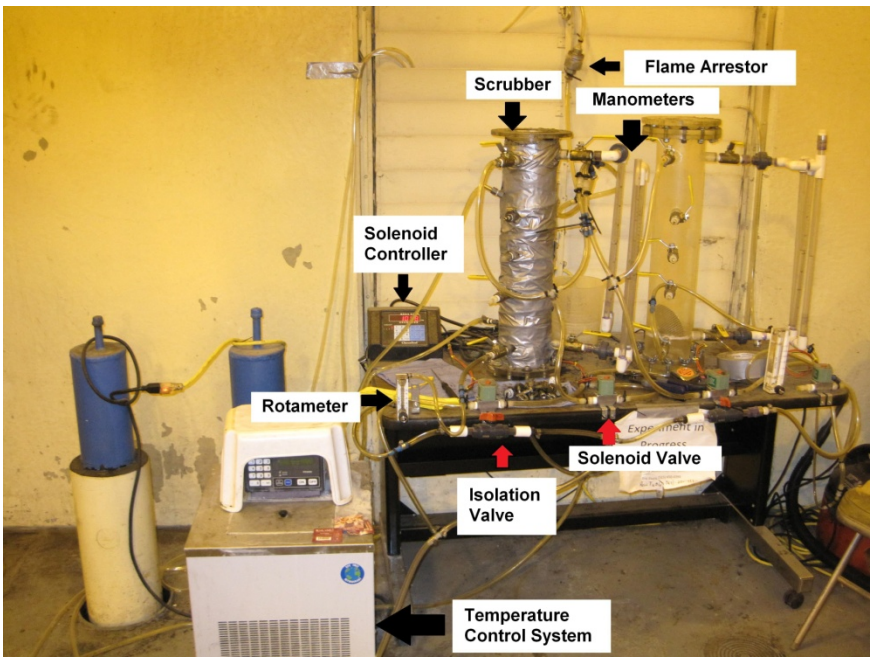

Figure 14, Scrubber system with the addition of the temperature control system

www.manaraa.com

Scrubber dimensions

The height of the screen supporting the media bed to the top lip of the scrubber was 53.5 cm. The media bed was generally 4,000 mL in volume and was approximately 42 cm in height. The diameter of the scrubber was 11.4 cm.

Temperature control system

As previously mentioned, the temperature control system consisted of a temperature controlled water supply, which was pumped into copper tubes that wrapped around the scrubber. The entire scrubber was also insulated. The temperature control system was used to test temperatures as low as 30°F (-1°C) and as high as 170°F (77°C). It should be noted that these temperatures are the temperature of the water supply. The actual temperature in the scrubber did not reach these temperatures. The data logging thermocouple measured the actual temperature in the scrubber during different trials.

The temperature control system was not added until Trial 16 of the experiments. It was at this time that the effect of temperature was to be studied and some method of changing the temperature inside the scrubber was necessary. Despite the lack of a temperature control system prior to Trial 16, the temperature in the scrubber remained fairly constant. This is primarily due to the location of the system in the Gas Handling Building. The Gas Handling Building contained engines which ran at peak hours to generate electricity from the biogas. The running of the engines created a fairly stable ambient temperature in the building. However, the system was also located next to a window in the Gas Handling Building. When outside temperatures reached extremes, it affected the temperature in the scrubber despite the use of a temperature control system.

Hydrogen sulfide detector

A Jerome® 860 hydrogen sulfide detector produced by Arizona Instrument LLC (Tempe, AZ) was used. The Jerome® 860 was a portable gas monitor that could continuously collect data and then transfer it to a computer or pocket PC via an infrared USB port. It was battery powered, water resistant, and safe. The detector used an electro-chemical sensor to measure H_2S concentrations. It was recommended that the measurement range be between 0 and 200 ppm, however the detector was able to handle occasional spikes in the H_2S concentration up to 1,000 ppm. The resolution of the detector was 0.2 ppm. It was recommended that the temperature of the measured gas be between 0°C and 50°C and the humidity of the gas be 20 to 80% for normal operation, but could reach 100%

www.manaraa.com

for short intervals. Oxygen was required for the sensor to operate properly, so between samples air was pumped through the sensor. (Arizona, 2005)

In high humidity and high temperature environments, it was recommended that the sensor be removed from operation every 2 days to allow the sensor to stabilize (Arizona, 2005). In the case of this experiment, the sensor was used for the entire 2.5 day time period for each trial. After the trial was complete, the sensor was removed from the system and air was run through the sensor until the next trial commenced.

Two-minute samples of gas from the inlet and outlet were taken every hour. An H_2S concentration was recorded every 2 seconds. The H_2S detector had the capacity to record 108,810 readings. In each trial, the system was run until the capacity of the H_2S detector was reached, which was about 2.5 days (60.5 hours).

Data logging thermocouple

The data logging thermocouple used was a ThermoWorks® (Lindon, UT) brand USB data logger (TW-USB-TC). It took a temperature reading from inside the scrubber every 30 seconds. The data logging thermocouple appeared to function correctly until Trial 19. It was then determined that the temperatures being recorded were inconsistent with the actual temperatures in the scrubber by comparing temperature readings from a dial thermometer in the scrubber. The data logging thermocouple was then sent back to the manufacturer and was replaced. The new data logging thermocouple was reinstalled and functioning correctly by Trial 26. During the time period where the data logging thermocouple was not available, temperature was recorded daily from the dial thermometer and averaged over the length of the experiment.

Rotameter

The rotameter used was manufactured by Omega Engineering, Inc. (Stamford, CT) and had the capability of measuring flows between 1 to 10 L/min of air at 0.5 L/min intervals. A correction for using biogas instead of air was used when calculating the actual flow rate of biogas through the system. Because of the specific gravity of the biogas, the correction of the biogas flow rate was calculated to be 1.0426 times the reading of the rotameter.

www.manaraa.com

Solenoid controller

The solenoid controller used was a model XT manufactured by ChronTrol Corporation (San Diego, CA). This controller could be programmed to control four solenoid valves. In the program for the controller used, 3 solenoid valves for taking samples of gas at various stages in the system and one air pump for stabilizing the detector were controlled. Because the scrubber system was initially designed for using 2 separate scrubbers, there are 3 solenoid valves built into the system for sampling gas: one to sample the inlet gas, and two to sample outlet gas from each of the two scrubbers. However, because only one scrubber was utilized in the actual study due to low biogas flow rates, only samples from two of the solenoid valves were used. A visual describing the program for the solenoid controller is shown in Figure 15.

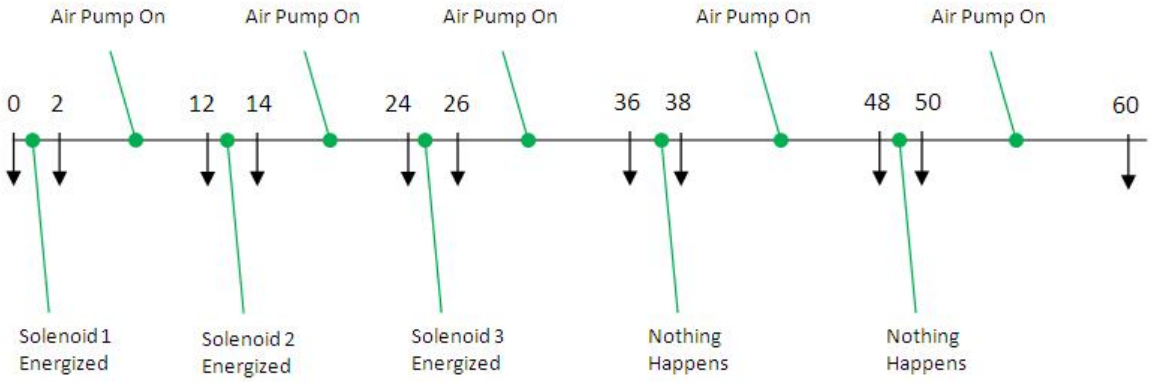

Figure 15, Solenoid controller program for a 60 minute cycle

In Figure 15, Solenoid 1 refers to the valve controlling sample gas from the inlet, Solenoid 2 controls the flow of sample gas from the first scrubber, and Solenoid 3 controls the flow of sample gas from the second scrubber. The air pump is energized during the times indicated and is only on when gas is not being sampled. The cycle was repeated every 60 minutes.

Flame Arrestor

The flame arrestor used was a Varec 5200 Flame Check, manufactured by Varec Biogas (Cypress, CA). A flame arrestor is designed to stop flashbacks in small pipe lines carrying flammable gases. It is recommended to be installed as close as possible to the open end of the pipe, where it is more likely a source of flame will originate. A flame arrestor extinguishes any flashbacks that are generated by passing it through a compressed woven wire element which absorbs heat from the

www.manaraa.com

flame faster than it is developed. The temperature is thus lowered below its ignition point and the flame is quenched.

Experimental Procedure

Material collection and measurement

TDRP and ORM were collected and weighed in Town Engineering Building on the Iowa State University campus. For almost all trials, 4,000 mL of TDRP was used. It was collected using a 4,000 mL beaker. The TDRP was manually mixed and large clumps were dispersed. The TDRP mass was then measured on a Model CW-11 floor scale manufactured by Ohaus Corporation (Pine Brook, NJ) and calibrated linearly with a zero point and a span point of 20 kg (subtracting the mass of the beaker, 0.32 kg); the scale was setup for a capacity of 100 kg with graduated increments of 0.02 kg. It should be noted that until Trial 10, the floor scale was not functional and there was no means of massing the TDRP. The masses of the TDRP prior to Trial 10 were estimated, depending on the method of collecting the media (mixing and sifting versus no additional mixing or sifting) and the bulk density of the TDRP.

Preparation of the experimental apparatus

The TDRP or ORM was poured into the top of the scrubber. A line was marked on the scrubber (see Figure 13) to show how high 4,000 mL of TDRP generally filled the scrubber. The bed height of the media was measured by measuring the distance from the top lip of the scrubber to the top of the bed and then subtracting it from the distance of the bottom of the media bed to the top lip (21-1/6”, or 53.5 cm). Any spilled TDRP was wiped off the top of the scrubber and vacuum grease was applied around the seal at the top. The lid of the scrubber was put in place, and the bolts were secured.

The data logging thermocouple was activated by connecting it to a computer via a USB port and using the software, EasyLog USB, to begin recording. The H_2S detector first needed to be calibrated in the labs at Town Engineering Building. Calibration gas of 200 ppm was most often used, but concentrations of 25 ppm and 10 ppm were also used. After calibration, the data already stored in the detector was cleared. The detector was then ready for data collection.

A system check was then performed to ensure that the appropriate valves were opened or closed and that the H_2S sensor and data logging thermocouple were recording.

www.manaraa.com

Beginning and running the experiment

After the system was checked, it was ready to begin an experiment. The gas was turned on. The flow rate through the system was controlled by the rotameter. To maintain a constant flow rate, it was found that a flow rate of 3 L/min or less resulted in a relatively flat system curve over the pressure range encountered. For most trials, a flow rate of 3 L/min was applied. Some trials focused on changing the empty bed contact time and these trials required different flow rates. The pressure in the line from the digester was recorded, as well as the inlet and outlet pressures from the manometers, the temperature from the dial thermometer, and the flow through the system.

After initial set-up and beginning of the experiment, the experiment was monitored on a daily basis. Pressure in the line from the digester was recorded, as well as the pressures from the manometers on the inlet and outlet end of the scrubber, temperature from the dial thermometer, and flow rate.

Occasionally, condensation in some of the plastic tubing was present. This was usually due to a temperature difference in the gas and the temperature control system. The tubes containing condensation were drained during the experiment to ensure that the water was not causing blockages.

Ending the experiment

After collecting approximately 2.5 days of data, the H_2S detector memory was exhausted and would automatically turn off. The data was then downloaded from both the H_2S detector and the data logging thermocouple. The scrubber was unsealed after the gas was shut off and the media was removed and disposed.

Siloxane Testing

Siloxane testing was conducted on inlet and outlet gas from the scrubber in order to evaluate the siloxane removal capability of TDRP (ORM was not evaluated for siloxane removal). Siloxane concentrations were measured concurrent with hydrogen sulfide testing. A small sample of inlet and outlet gases was drawn from the lines; no effect on flow was observed.

The methods described by Air Toxics (Saeed, Kao , & Graening, 2002) were used for siloxane sampling and analysis of type D4 (Octamethyl-Cyclotetrasiloxane) and type D5 (Decamethyl-

www.manaraa.com

Cyclopentasiloxane) siloxanes. Results are reported as the sum of D4 and D5 siloxanes. The specific methods and equipment for this test are described in Appendix II.

Site Variables

There are a number of variables that control the site conditions for this study. A brief explanation of each variable can be found below.

Flow Rate of Biogas

The flow rate of the biogas through the system was controlled by the pressure at the gas tap of the anaerobic digesters. The pressure varied between 14"-16" at the gas tap which, after losing some pressure head along the line to the experimental apparatus, gave a maximum flow of between 3-6 L/min. The flow of the gas through the system was controlled by a rotameter (up to the maximum flow) which was connected to the scrubber. The original research plan indicated that a flow of 2.7 cubic feet/min (76.5 L/min) would be used, but this flow was scaled back to meet site specific conditions.

The flow rate of the biogas and the height of the media bed determine the residence time, or empty bed contact time. Using a full bed of media (defined as 4,000 mL and explained further below), the empty bed contact time varied from around 60 seconds to around 500 seconds.

Amount of Media

The amount of media used was measured volumetrically. For a "full bed" in the scrubber, 4,000 mL of media was used. This volume of media gives a mass of between 1,340 to 1,580 grams. A few of the trials used a "half-bed" of media, which was 2,000 mL of TDRP.

Type of Media

There were two types of waste rubber materials available for use in this study. From knowledge passed on from Envirotech, Inc., ORM contained slightly coarser particles and no metal additions. TDRP was finer and had metal additions, supposedly from the steel belts of the discarded tires. A previous study showed that iron, calcium, zinc, and magnesium were present in TDRP, but the exact quantities were unknown. Additional characterization of TDRP and ORM from a previous study can be found in the Literature Review section. Most of the experiments in this study focused on using TDRP. However, there were 5 trials performed at the end of the study using ORM.

www.manaraa.com

Traditionally, activated carbon or steel wool is used as an adsorbent for hydrogen sulfide in similar applications. As a comparison, two experiments were done using steel wool as the media and one experiment was run as a blank, using marbles as an inert surface for the gas to pass through.

Compaction of Media

TDRP is capable of being significantly compacted. Most of the experiments used TDRP in its loose, natural form, with no additional compaction other than from the weight of itself. However, a few trials focused on the effects of compacting the media. The method of compaction was to apply pressure at the top of the bed using manual force and then placing glass marbles on top of the media to prevent it from expanding. In the compaction trials, the bed was compacted to up to 66% of its original volume.

Temperature

The temperature of the gas in the system was primarily a function of the temperature of the gas leaving the anaerobic digesters or the temperature inside the Gas Handling Building. When the temperature control system was not in operation, the temperature inside the scrubber appeared to be a function of time and ran in a daily, cyclical cycle that did not necessarily correlate with the weather (day vs. night).

Concentration of the Inlet Gas

The concentration of the biogas from the anaerobic digesters varied. It was usually between 250-300 ppm, but got as high as 1,600 ppm and as low as 60 ppm. There were sometimes drastic drops in the concentration that appeared to correlate with fat, oil, and grease (FOG) deliveries from a large local restaurant, Hickory Park. It was not possible to control inlet concentration. A value that has been developed to characterize the amount of hydrogen sulfide loading to the scrubber is the mg of H_2S present in the gas per gram of TDRP present in the media bed per hour. The Results section contains a plot of H_2S concentrations from all experiments over the course of approximately 10 months (Figure 20).

Pressure

The atmospheric pressure is used to calculate the amount of hydrogen sulfide removed. The atmospheric pressure is slightly variable, but is usually very close to 1 atm. The values used for atmospheric pressure are taken from the Weather Underground (www.wunderground.com).

www.manaraa.com

CHAPTER 5. RESULTS AND DISCUSSION

Hydrogen Sulfide Testing

Various operational conditions were tested to determine their effect on the hydrogen sulfide (H_2S) concentration of the outlet gas. The following conditions were tested:

- Empty bed contact time
- Temperature of the biogas and scrubber media
- Compaction of the media bed
- Mass of TDRP used in the media bed

Two different types of waste rubber materials were used from Envirotech Systems, Inc.: tire derived rubber particles (TDRP) and other rubber materials (ORM). Most of the experimental testing on different operational conditions was done using TDRP. ORM was only tested at a single empty bed contact time, temperature, compaction (density), and mass.

A typical breakthrough curve from this study is shown in Figure 10. Breakthrough occurred when the H_2S concentration in the outlet gas began to increase. In this section, two different time periods are referred to: the time from the start of the experiment until the point of breakthrough, and a fixed period of time for all experiments that was from when the experiment began until it was ended, and always exceed the time until breakthrough.

Empty bed contact time

Empty bed contact time was varied by adjusting flow to the scrubber using a rotameter equipped with a needle valve. A longer contact time was found to slightly increase the amount of H_2S removed up until the time of observed breakthrough, although the total amount of H_2S removed throughout the duration of the experiment was not found to be dependent on the contact time. This suggests that there was a maximum amount of H_2S that could be removed by the TDRP particles as a result of thermodynamic limitations. To overcome kinetic limitations, a longer contact time resulted in greater H_2S removal prior to reaching maximum removal capacity. These findings can be seen in Figure 16.

www.manaraa.com

As a statistical analysis, F-tests which tested the research hypothesis that the slope of the trendline, β, was 0 were performed. These F-tests tested the null and research hypotheses as listed in Eq. 26.

$$H_o: \beta = 0 \; vs. H_a: \beta \neq 0 \qquad \text{(Eq. 26)}$$

Two F-tests were performed. The first F-test tested whether there was a trend in the data for the amount of H_2S adsorbed from the starting time of the experiment up until the point of breakthrough. The second F-test tested whether there was a trend in the data for the amount of H_2S adsorbed from the starting time of the experiment until the end of the experiment, which was a fixed amount of time for all experiments.

For the first F-test, the trend of H_2S removed at breakthrough was found to be statistically significant (see Table 4 for results of statistical tests), meaning that the research hypothesis that the slope was 0 was rejected at α=0.25. On the other hand, the second F-test found that the H_2S removed over a fixed period of time did not vary as a function of empty bed contact time; i.e. fail to reject the hypothesis that the slope is zero (Table 4). Therefore, there was not a trend over this data and there was evidence that the empty bed contact time did not change the total amount, which included H_2S adsorbed after breakthrough, of H_2S adsorbed over an extended period of time. The p-values of the statistical tests can be used to test significance under different values for α. If the p-value is less than the chosen α-value, it is a good indication that the null hypothesis can be rejected at that α-value.

Table 4, Statistical test results for empty bed contact time

Data	F-test	R^2	F_c	$F_{0.25,1,4}$	p-value
Adsorbed until breakthrough	#1	0.72	10.2	1.81	0.03
Adsorbed over fixed time	#2	0.12	0.56	1.81	0.49

www.manaraa.com

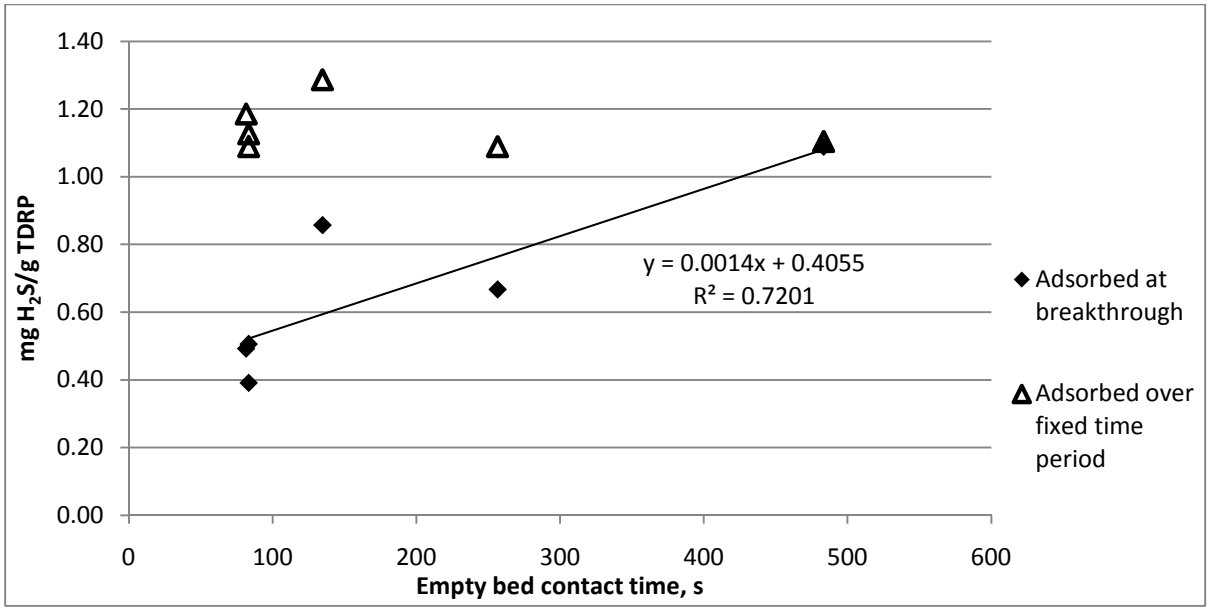

Figure 16, Effect of empty bed contact time on H_2S removed at breakthrough and over a fixed time period

Appendix I contains the complete data set for the trials that are associated with Figure 16.

Temperature

The effect of temperature on adsorption was tested. Figure 17 shows the relationship between temperature in the scrubber and the total amount of H_2S removed over a fixed period of time. Low temperatures were tested by setting the temperature control system to 30°F (-1°C). Medium temperatures were tested either at ambient temperatures (which was around 75°F (24°C) in the Gas Handling Building) before the temperature control system was installed, or after it was installed the temperature control system was set to 75°F (24°C). High temperatures were tested by setting the temperature control system to 170°F (77°C).

In the tests performed, low temperatures appeared to have the highest H_2S removal capacity; however, the data did not identify a significant effect of temperature. The low correlation (R^2=0.0046) of this trendline signified the lack of a trend between temperature and H_2S removal capacity. A statistical F test for determining whether the slope of the trendline was zero concluded that there was no evidence that there was a linear trend among the data (Table 5). Kohl and Nielsen (1997) indicate that the adsorption process is always exothermic, and therefore adsorption capacity decreases with increasing temperature. This may be the correct trend for TDRP and the relatively small amount of H_2S removed at medium temperatures could be due to the lower concentrations of H_2S in the inlet gas. The average inlet H_2S concentration for the medium temperature trials was 355

www.manaraa.com

ppm, whereas the average inlet H_2S concentration for the low temperature, which exhibit higher removal capacities, was 637 ppm. Figure 21 shows the trend between inlet H_2S concentration (described as H_2S loading) and H_2S removal capacity. Because the H_2S removal capacity appeared to be lower at higher temperatures, this indicated that kinetics was not a limiting factor for the reaction between the H_2S and TDRP and therefore an increase in temperature, which would increase the kinetic rate of reaction, was not beneficial in achieving maximum H_2S removal. This indicated that the equilibrium between H_2S and TDRP, instead of the kinetics, governed H_2S removal from biogas using TDRP as the adsorbent. However, there was not a large difference in the temperatures that were tested, and the effect of temperature may not be clearly seen in the range of temperatures that were used. Future tests on much higher or lower temperatures, if possible, could yield a significant trend.

Table 5, Statistical test results for temperature effect

Data	R^2	F_c	$F_{0.25,1,10}$	p-value
Temperature	0.0046	0.06	1.49	0.82

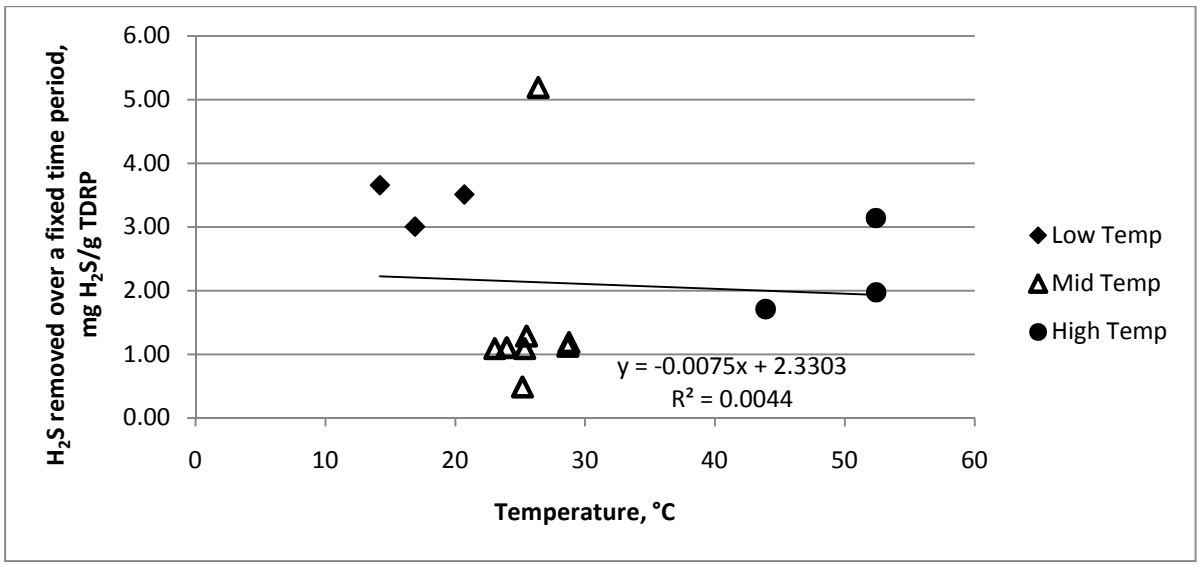

Figure 17, Effect of temperature on the amount of H_2S removed over a fixed time period

Appendix I contains the complete data set for the trials that are associated with Figure 17.

Compaction

The effect of compaction on the media bed was tested. The same initial mass of TDRP was used (approximately 1.4 kg) in each test. After being placed in the scrubber, the bed was compacted

www.manaraa.com

to approximately 65% of the volume of the original bed in both trials (from 4,000 mL to 2,600 mL). The results show that, in general, compaction improved adsorption capacity (Figure 18). The trendline gave an R^2 value of 0.432. A statistical F test for determining whether the slope of the trendline is zero concluded that there was evidence that there was a linear trend among the data (Table 6). It was hypothesized that the improved capacity resulted from reduced biogas short-circuiting. The average H_2S removed with compaction was 1.89±0.45 mg/g TDRP, whereas the average removed without compaction was 1.13±0.05 mg/g TDRP.

Table 6, Statistical test results for compaction effect

Data	R^2	F_c	$F_{0.25,1,10}$	p-value
Compaction	0.432	3.80	1.69	0.109

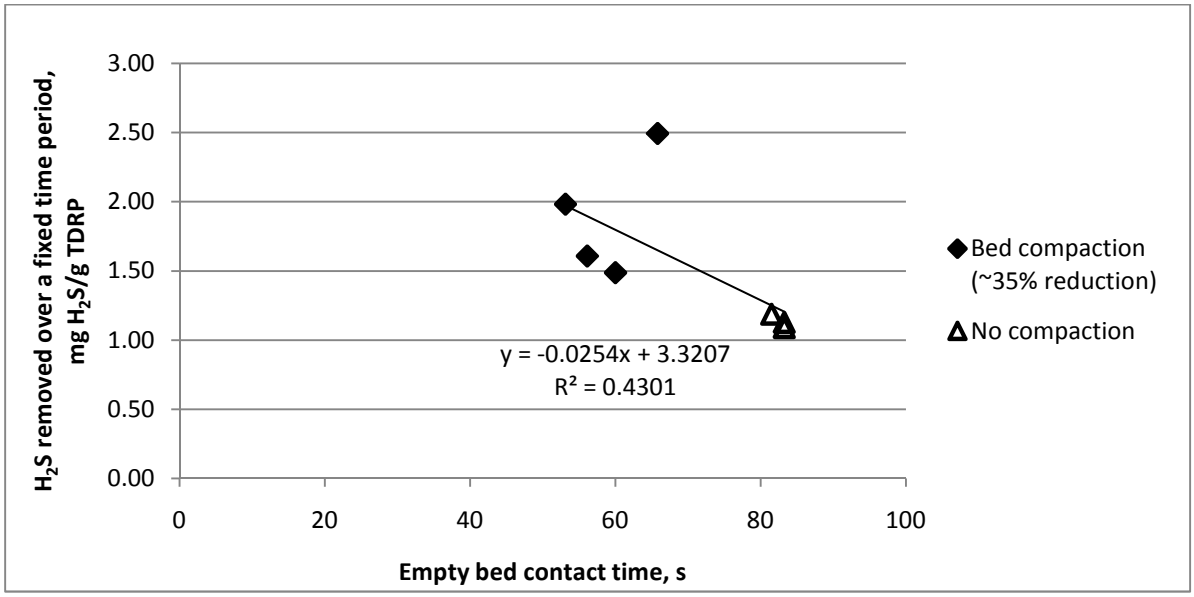

Figure 18, Bed compaction effects on amount of H_2S removed

Appendix I contains the complete data set for the trials that are associated with Figure 18.

Mass of media bed

Reducing the mass of the media bed decreased the amount of H_2S that was removed on a mass of sulfur per mass of TDRP basis. This is shown in Figure 19, where the flow rate was the same for both the full bed (4,000 mL) and half bed (2,000 mL) trials and the density was maintained at its uncompacted density.

www.manaraa.com

Table 7, Statistical test results for effect of mass of media

Data	R^2	F_c	$F_{0.25,1,3}$	p-value
Mass of media bed	0.888	15.84	2.02	0.058

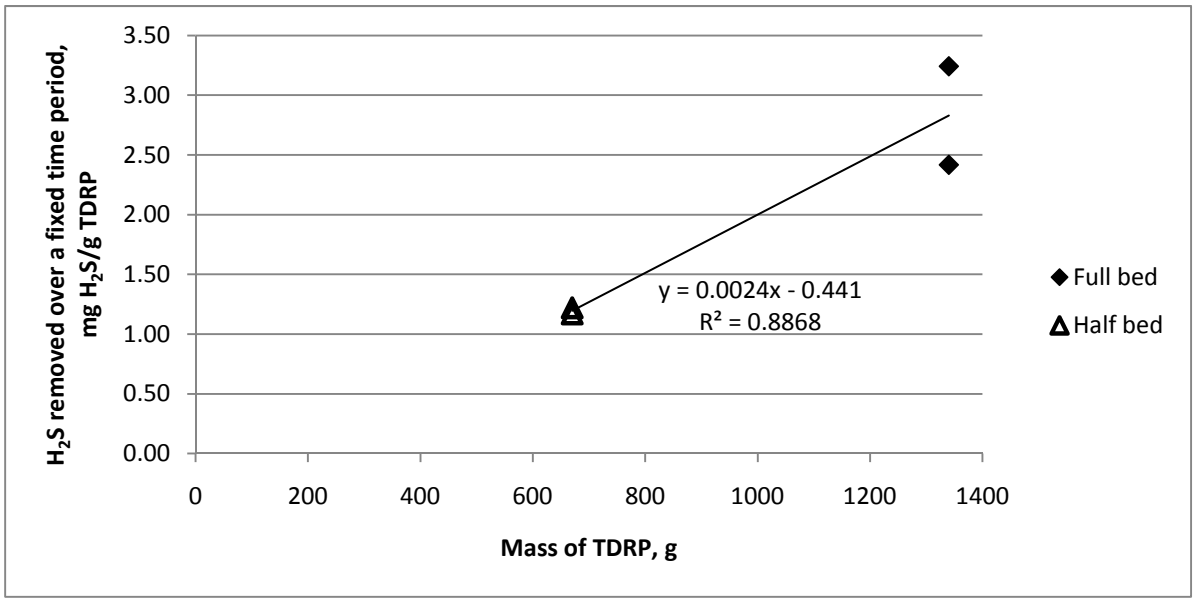

Figure 19, Effect of the mass of the media bed on the amount of H_2S removed

A full bed had an average mass of approximately 1,400 g, and a half bed had approximately half of that mass. Figure 19 shows that the amount of H_2S removed from the biogas was dependent on the mass and volume of TDRP present. The change in removal capacity in the half bed may have been due to a decrease in the contact time, and therefore, related to the adsorption reaction time.

Appendix I contains the complete data set associated with Figure 19

Variation of inlet H_2S concentration

Hydrogen sulfide concentration in the biogas from the WPCF was not constant, even over a 2.5 day trial. Figure 20 shows how the inlet H_2S concentration changed over the time period that experiments were being run. A vertical spread of data indicates the range of H_2S concentrations over one run. Input of fats, oils, and greases (FOG) strongly affected hydrogen sulfide concentrations. FOG deliveries from Hickory Park, a local restaurant, were recorded and compared to hydrogen sulfide concentrations. Following FOG deliveries, the hydrogen sulfide concentration dropped precipitously (over the course of one hour) as shown in Table 8. This effect may be explained by increases in methane and carbon dioxide production leading to the dilution of hydrogen sulfide.

www.manaraa.com

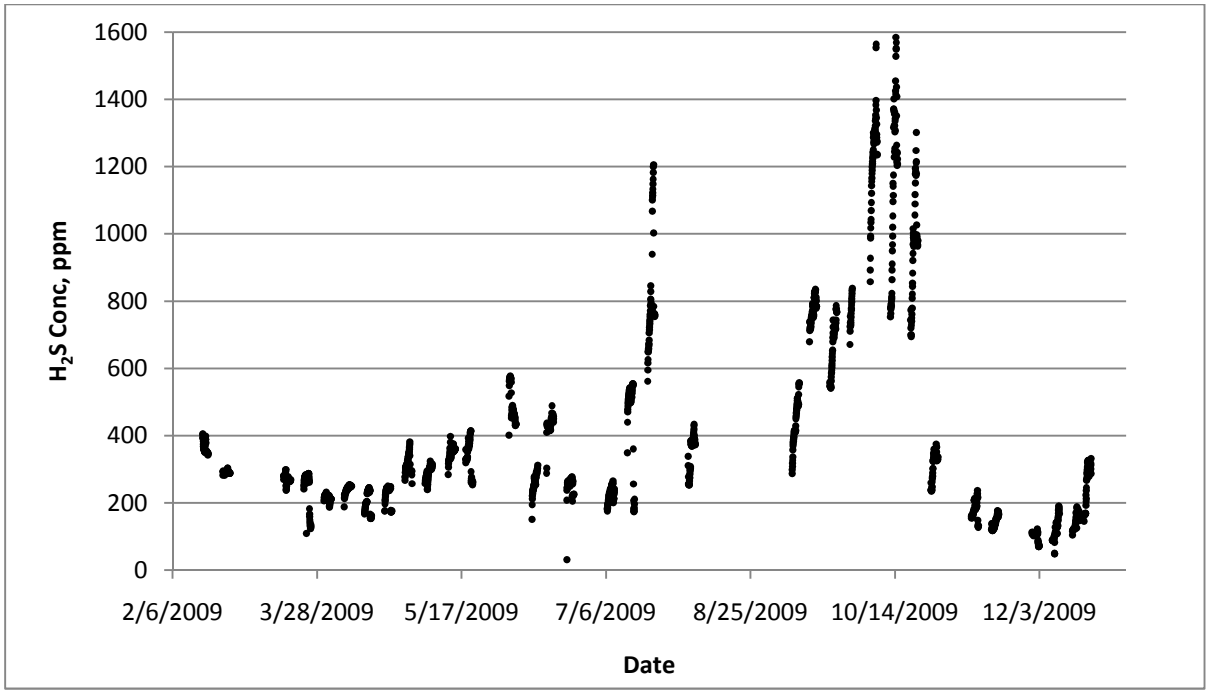

Figure 20, Inlet H_2S concentration over the time period when experiments were run

Table 8, Observed effect of FOG delivery on Ames WPCF Digester H_2S concentration

FOG Delivery Date	FOG Source	H_2S Concentration Before Delivery, ppm	H_2S Concentration After Delivery, ppm
3/26/2009	Hickory Park	262	125
5/20/2009	Hickory Park	414	261
7/15/2009	Hickory Park	551	175
10/21/2009	Hickory Park	1302	981
12/2/2009	Hickory park	114	70

Additionally, it was found that the higher the inlet concentration of H_2S, the higher the amount of H_2S removed from the biogas. A higher inlet concentration means that there is a higher partial pressure of H_2S in the gas stream, which, as discussed in the Theory section, has been found to increase adsorption. Figure 21 shows this effect in terms of the amount of H_2S loading on the media versus the amount of H_2S removed per gram of media. The flattening of this plot supports the observation that the maximum adsorption capacity lies in the range between 3 and 5 mg H_2S/g TDRP or ORM.

www.manaraa.com

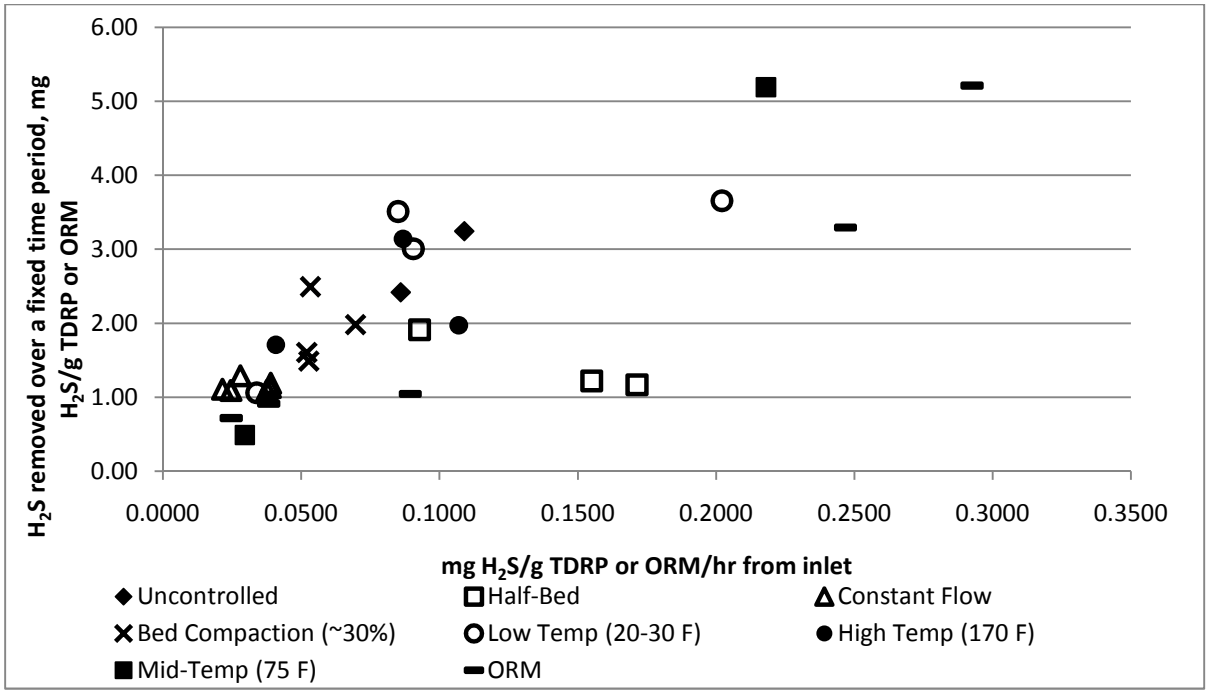

Figure 21, Relationship between H_2S loading and specific H_2S removal

Pressure Drop

The flow of biogas through the media bed caused a pressure drop across the bed. Figure 22 shows the pressure drop over the depth of the media bed versus the flow of biogas through the system. As can be seen in Figure 22, it appears as if increasing the flow of biogas through the system caused an increase in pressure drop over the depth of the media bed.

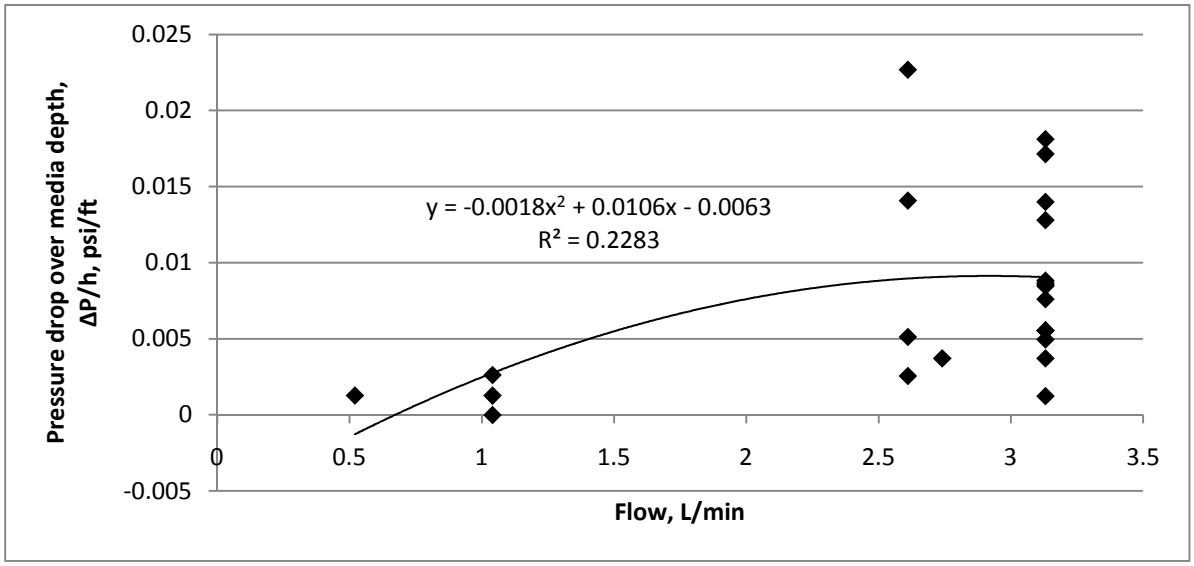

Figure 22, Pressure drop over the depth of the media bed (psi/ft) vs. flow of biogas through the system

www.manaraa.com

Comparison to other adsorbents

Hydrogen sulfide adsorption on other materials was tested in the scrubber system to serve as a comparison to TDRP and ORM. Steel wool, a known H_2S adsorbent, was tested in two trials. In the trials using steel wool, breakthrough was immediate. After the first trial, the mass of steel wool used was increased and the flow rate was decreased (so as to increase the empty bed contact time), but breakthrough still occurred immediately. Therefore, under the environmental conditions present in this study, TDRP and ORM were much better adsorbents of H_2S.

Glass beads, which served as an inert surface, were also tested for one trial. Breakthrough occurred immediately, although approximately one third of the way through the experiment the beads began to show some capacity for H_2S removal. This was thought to be due to water condensation on the surface of the glass beads. Hydrogen sulfide can dissociate in water and is therefore removed from the gas stream. This effect was also seen in other experiments where the saturated media still appeared to be removing H_2S from the biogas (as can be seen in the gap between inlet and outlet H_2S concentrations at the end of the experiment shown in Figure 10). To remove the amount of H_2S thought to be due solely to condensation in Figure 10, about 81 mL of water condensation would be needed.

Data for these trials can be found in Appendix I.

Siloxane Testing

The effect of TDRP on siloxane (D4 and D5) removal was evaluated by sampling the biogas before and after the scrubber (Table 9). For the first four tests, only inlet gas was sampled to establish the background concentration, because only one sampling system was available. Based on the results, the TDRP apparently removed in excess of 98% of the siloxanes from the biogas. ORM was not tested for siloxane removal.

www.manaraa.com

Table 9, Siloxane concentrations in biogas and outlet biogas from TDRP scrubber

Date	Biogas Siloxane Concentration, mg/m^3	Scrubber Outlet Biogas Siloxane Concentration mg/m^3
4/25/2009	10.2	NT[A]
5/13/2009	1.12	NT
5/14/2009	0.72	NT
5/18/2009	3.59	NT
7/20/2009	75.6	1.32
8/4/2009	91.9	0.310
Average ± Standard Deviation	30.52 ± 41.69	0.815 ± 0.714

[A]NT = not tested

Isotherm Modeling

Freundlich Isotherm

Using Eq. 24, the Freundlich Isotherm can be fit to experimental data for ORM and TDRP. Values for C_e and X_{sat} were taken from the raw data, converted to appropriate units, and plotted using Eq. 24. The results can be seen in Figure 23 and Figure 24. The data used for Figure 23 and Figure 24 were chosen because of the similar operating conditions in each trial. These operating conditions included a biogas flow rate near 3 L/min, no compaction, a TDRP or ORM bed volume of 4,000 mL (therefore similar masses of TDRP or ORM), and temperature. "Isotherm" means the temperature is held constant. In each of the trials used for the determination of Figure 23 and Figure 24, the temperature was relatively constant, around 25°C ± 3°C.

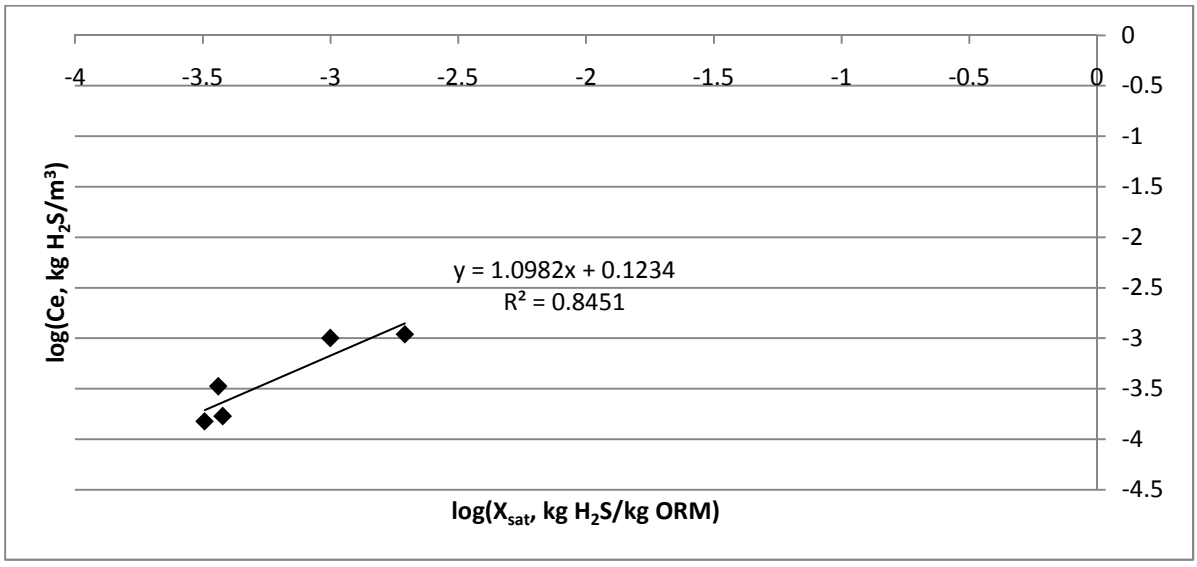

Figure 23, Freundlich Isotherm modeling of ORM at 25°C

www.manaraa.com

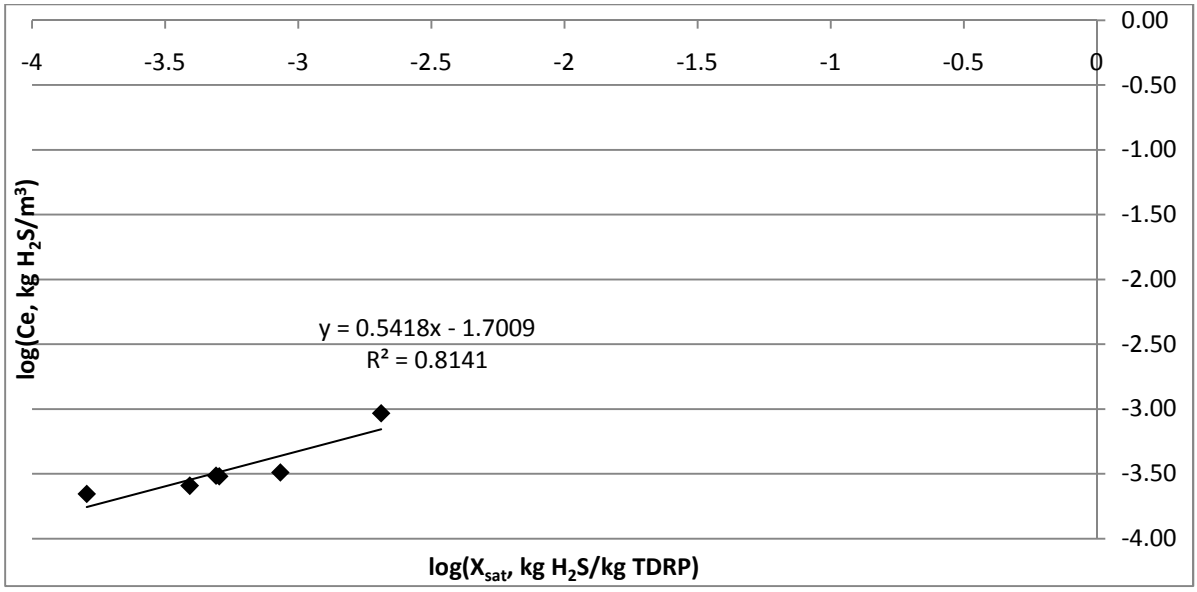

Figure 24, Freundlich Isotherm modeling of TDRP at 25°C

The raw and converted data used in Figure 23 and Figure 24 can be found in Appendix I.

Using the slopes and y-intercepts of Figure 23 and Figure 24, α and β values for ORM and TDRP were calculated. These results are shown in Table 10.

Table 10, Freundlich Isotherm constants at 25°C

	α	β
ORM	1.328	1.098
TDRP	0.020	0.542

The same method as described above was used to analyze the isotherms at other temperatures. As described in the Materials and Methods section, the temperature control system was set at 30°F/-1°C and 170°F/77°C for three experiments each on TDRP. These settings translated to temperatures in the scrubber of 14-20°C and 44-52°C. Using data at these approximate temperatures, isotherms for "low" and "high" temperatures were created and the Freundlich Isotherm models for TDRP can be seen in Figure 25 and Figure 26. Data used for both of these figures can be found in Appendix I.

www.manaraa.com

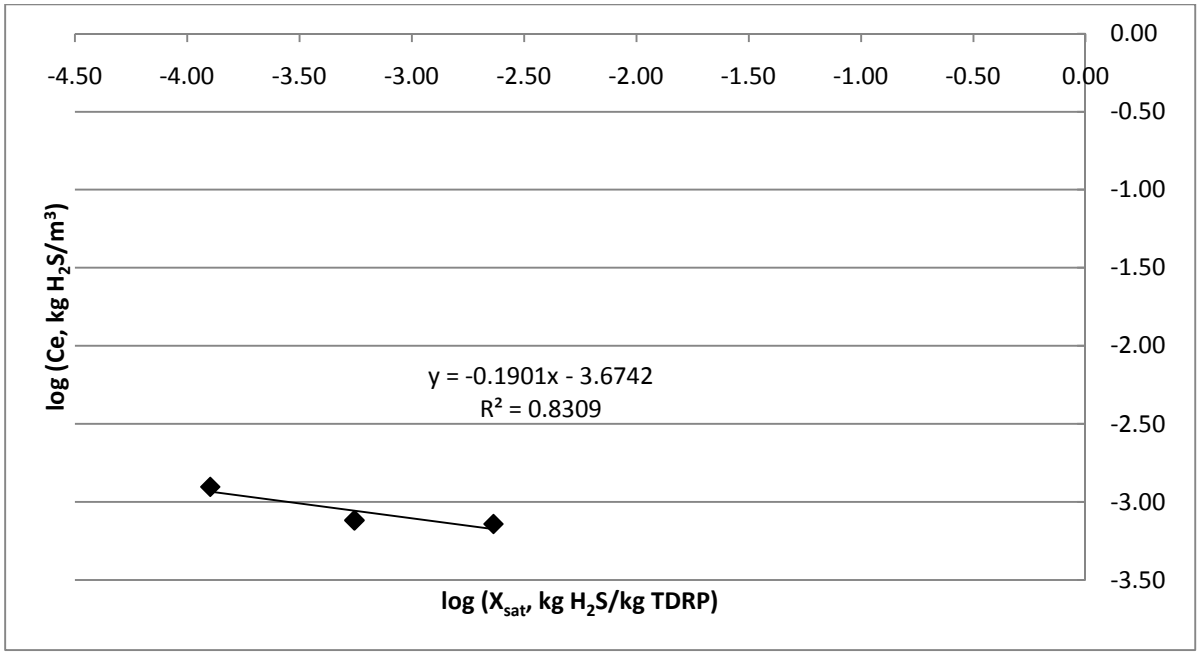

Figure 25, Freundlich Isotherm modeling for TDRP at 14-20°C (low temperatures)

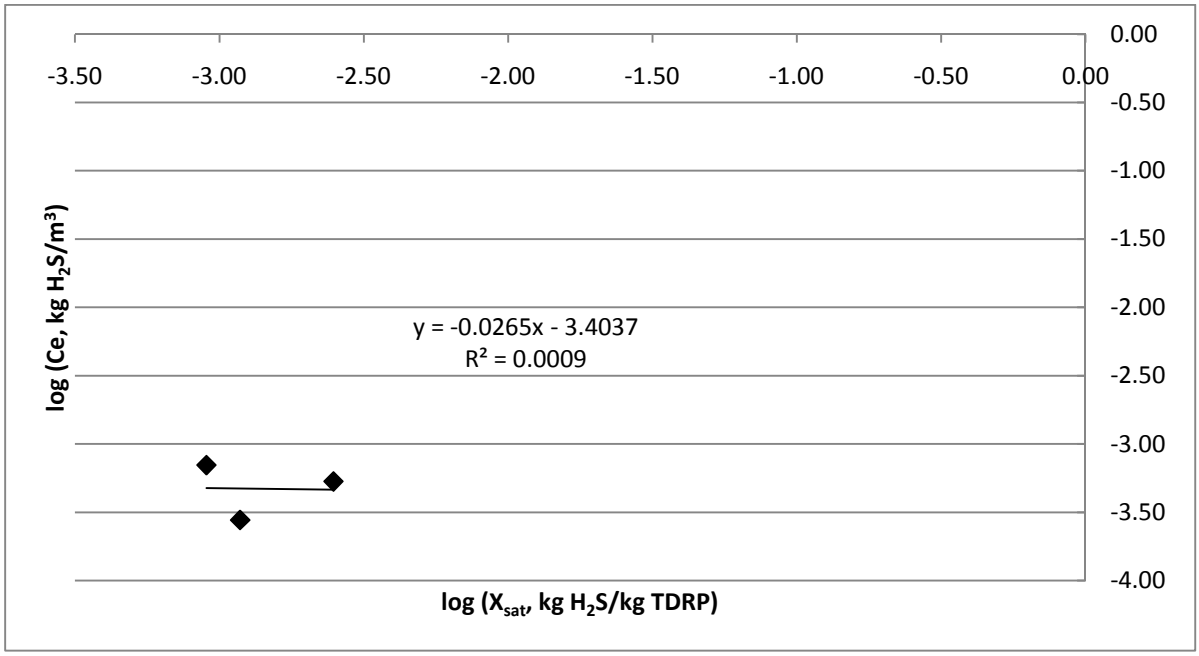

Figure 26, Freundlich Isotherm modeling for TDRP at 44-52°C (high temperatures)

Figure 25 for low temperature shows a satisfactory correlation of the Freundlich model to the data. However, Figure 26 for high temperature shows a very poor correlation of the model to the data. Unfortunately, due to time constraints, additional data for high temperature was not able

www.manaraa.com

to be collected. The α and β Freundlich constants were calculated for low temperature, but not at high temperature, due to the lack of correlation of the model to the data. The constants for low temperature are shown in Table 11.

Table 11, Freundlich Isotherm constants for TDRP at 14-20°C (low temperature)

	α	β
TDRP	2.117E-4	-0.190

Langmuir Isotherm

The Langmuir Isotherm was also used to model the data. While the Freundlich Isotherm is common for modeling experimental data due to its log-log determination of constants, the Langmuir Isotherm does not model the data as easily. However, if the Langmuir Isotherm is a good fit to the experimental data, then there is further evidence that the H_2S adsorption occurs in a monolayer over the media. The data was modeled according to the Langmuir Isotherm described by Eq. 16. The isotherms for ORM and TDRP at 25°C can be seen in Figure 27 and Figure 28.

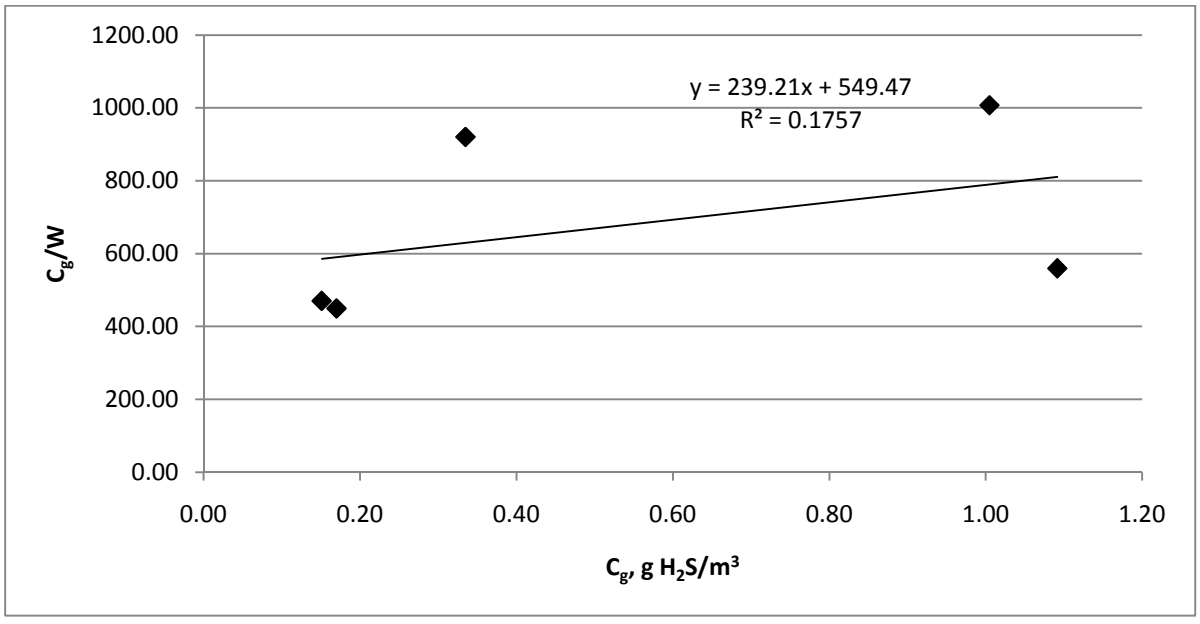

Figure 27, Langmuir Isotherm modeling of ORM at 25°C

www.manaraa.com

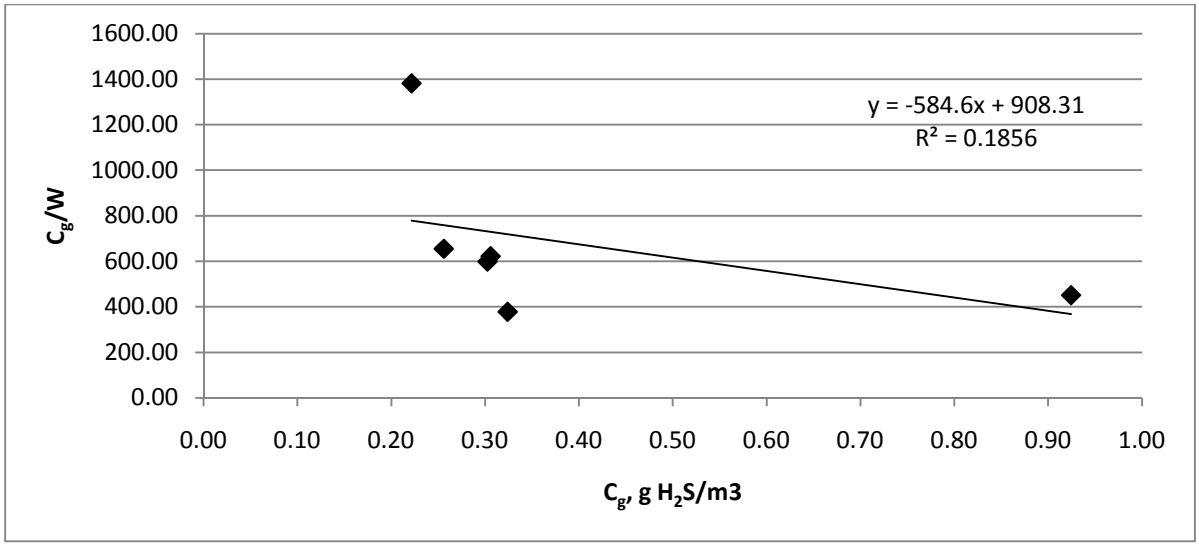

Figure 28, Langmuir Isotherm modeling of TDRP at 25°C

As can be seen in Figure 27 and Figure 28, the Langmuir Isotherm does not appear to be a good fit for the experimental data at 25°C. This could be because the adsorption is not monolayer, or because it is experimental data and other conditions interfered with the results. Figure 29 and Figure 30 show the Langmuir Isotherm fit to the data at low temperature (14-20°C) and high temperature (44-52°C). The Langmuir Isotherm appears to be a much better fit at low temperatures. This suggests that adsorption may actually be monolayer and that the discrepancies seen in the model fit at 25° may be due to the interference of other experimental conditions. However, only 3 data points were collected at both low and high temperatures and therefore the differences in the model fit may also be due to the lack of sufficient data.

www.manaraa.com

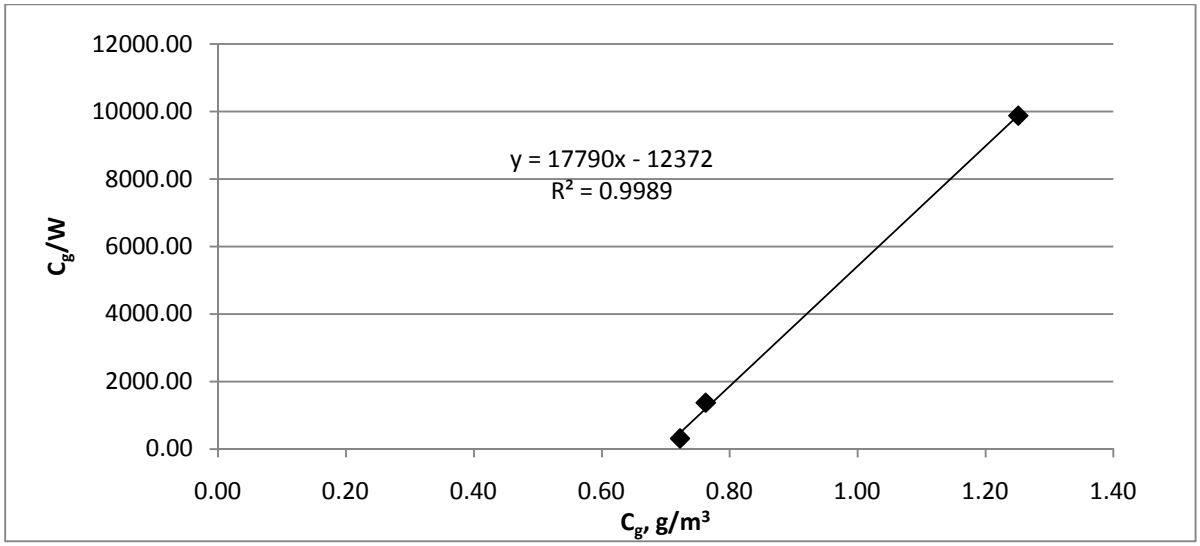

Figure 29, Langmuir Isotherm modeling of TDRP at 14-20°C (low temperature)

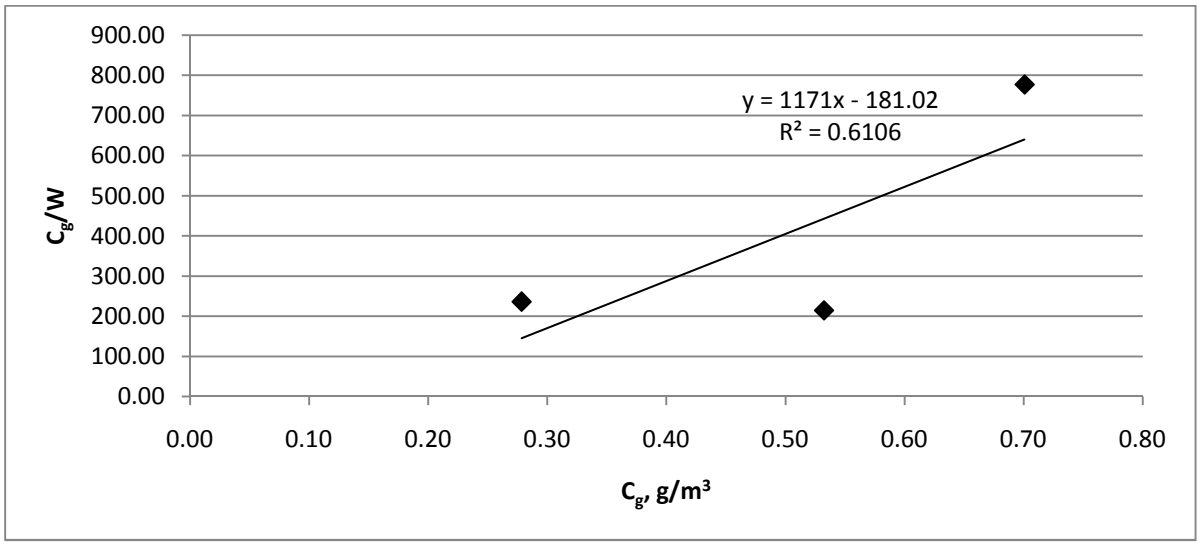

Figure 30, Langmuir Isotherm modeling of TDRP at 44-52°C (high temperature)

B.E.T. Isotherm

As described in the Theory section, the B.E.T. Model is used to model adsorption when there are multiple layers of adsorbate molecules on the adsorbent surface. The B.E.T. Model is described in Eq. 17. However, as also described in that section, the B.E.T. Model is difficult to evaluate when the ratio of the partial pressure of the adsorbate in the gas stream to the vapor pressure of the adsorbate at the system temperature is less than 0.05. This ratio was calculated to be approximately 8.5×10^{-3} for the highest concentration measured over the course of this study, 1600 ppm. Therefore, it was not attempted to fit this model to the experimental data.

www.manaraa.com

CHAPTER 6. ENGINEERING SIGNIFICANCE

The theoretical model described by Eq. 25 in the Theory chapter (and shown again below) confirmed the experimental results in terms of the effects of empty bed contact time, temperature, and compaction (bulk density) on hydrogen sulfide removal. As seen in Eq. 25, decreasing the flow rate ($\dot{m}_a$), which increases the empty bed contact time, will decrease the volume of media needed to satisfy a certain breakthrough time requirement. Therefore, the adsorption capacity of the media increases. Compacting the media, which increases the bulk density of the adsorbent, ρ_{ad}, will also increase the adsorption capacity. Eq. 25 is based on an isotherm, where different α and β constants will be needed at different temperatures. Concentration of H_2S in the inlet biogas, C_0, will increase the volume of media needed. This is consistent with experimental data, except that this equation does not take into account that higher H_2S loading will also lead to increased adsorption capacity for H_2S, with a maximum of between 3-5 mg H_2S/g media. In addition, this model does not take into account the variation of inlet concentration, flow, or temperature over time. Other rubber material (ORM) was only tested at a single empty bed contact time, temperature, and density, but the theoretical model can also be applied to ORM.

$$Volume = SF \cdot AD_b = SF \cdot \frac{\dot{m}_a t_B}{\rho_a \rho_{ad}} \alpha^{1/\beta} C_o{}^{(\beta-1)/\beta} \qquad \text{(Eq. 25)}$$

These results can help to predict the volume of media needed for a specific application, and can lead to a more economical process.

System Sizing

Because the Freundlich Isotherm best modeled the experimental data, it was used as a basis to size an adsorption system using ORM and TDRP. Equation 25 was applied to determine the appropriate volume of TDRP or ORM necessary for H_2S removal from biogas at a facility such as the WPCF. According to the biogas study performed in 2006 for the WPCF, biogas has a specific density of 0.92 with respect to air. Air at 25°C (the average temperature of the biogas during the experiments) has a density of 1.184 kg/m^3. This gives a biogas density of 1.089 kg/m^3. It should be noted that the width of the adsorption zone, δ, was assumed to be zero for ease of calculation and instead a safety factor was applied to avoid sudden breakthrough. Using Eq. 25 and inputting biogas flow rate, inlet H_2S concentration, density of the TDRP or ORM (depends on the extent of compaction), the desired breakthrough time, and the appropriate α and β values from Table 10

www.manaraa.com

produced Eq. 27, which gives the necessary volume of TDRP that will be required when the gas is 25°C.

$$Volume\ TDRP\ or\ ORM = SF \cdot \frac{V_b t_B}{1000\rho_{ad}} \alpha^{\frac{1}{\beta}} \left(\frac{1.39C}{10^6}\right)^{(\beta-1)/\beta} \quad \text{(Eq. 27)}$$

In Eq. 27, V_b is the biogas flow rate in L/min, C is inlet concentration of H_2S in ppm, t_B is the desired breakthrough time of the system in minutes, and ρ_{ad} is the density of the TDRP in kg/m^3. The volume of TDRP required is in m^3.

From the Ames WPCF Digester Gas Improvements Study, it was estimated that the anaerobic digesters produce about 56,800 ft^3 of biogas per year. To estimate the size of an H_2S removal system needed at the WPCF using TDRP or ORM, a few assumptions were made when using Eq. 7. If the biogas production is averaged evenly over a course of a year, a flow of 3.06 L/min of biogas comes from the digesters. From looking at Figure 20 it seems as if the inlet concentration of H_2S was most often around 300 ppm. The density of ORM was taken to be 250 kg/m^3 and TDRP was 375 kg/m^3, which are approximately in the middle of the ranges of TDRP/ORM densities. If the desired breakthrough time was one year, then the approximate volume of ORM and TDRP needed would be 4.16 m^3 and 2.26 m^3, respectively. Inlet H_2S concentration, biogas flow, and temperature may be variable in actual system conditions, and therefore a safety factor should be used in order to prevent premature breakthrough. If a safety factor of 3 is used, then approximately 12.48 m^3 of ORM or 6.77 m^3 of TDRP would be needed on a yearly basis. Dimensions of the scrubber system could be chosen to fit the necessary volume.

The volume of TDRP required would be different if a different temperature in the scrubber is maintained. The concentration conversion from ppm to kg/m^3 would change to 1.43E-6 at low temperature (average temperature is 17°C) from 1.39E-6 at 25°C. Using the Freundlich constants from Table 11, an assumed flow rate of 3.06 L/min of biogas, an inlet H_2S concentration of 300ppm, and a TDRP density of 375 kg/m^3, the volume of TDRP necessary for one year of H_2S adsorption at the WPCF is 0.08 m^3. When a safety factor of 3 is used, then approximately 0.23 m^3 of TDRP would be needed. Economically, the smaller amount of media needed at a lower temperature must be balanced against the cost of cooling the gas to a lower temperature.

www.manaraa.com

The validity of this model can be checked by using Eq. 25 to predict the volume of media needed under certain conditions and then comparing the predicted volume with the actual volume used. For TDRP using the Freundlich Isotherm, Table 12 is the volume of TDRP used in the experiment compared to the predicted volume of TDRP needed for breakthrough to occur under the operational conditions in each trial, which is found by imputing mass flow rate, bulk density of TDRP, average inlet concentration, and time until breakthrough occurred. No safety factor was added to the calculation of predicted volume. Additionally, the width of the adsorption zone was assumed to be zero, which could introduce some error into the calculation. The trials shown are the same trials used to determine the Freundlich constants for TDRP at 25°C.

Table 12, Measured vs. predicted volume of TDRP needed using experimental data

Trial	Measured volume of TDRP, mL	Volume of bed, mL	Predicted volume, mL	% difference
7	4000	4291	4765	16
8	4000	4291	7233	45
9	4000	4291	5434	26
10	4000	4291	5177	23
23	4000	4355	2506	-60
34	4000	4436	3170	-26
Average	**4000**	**4326**	**4714**	**4**

The "Measured volume of TDRP" is the volume of TDRP that was measured using a beaker. The "Volume of bed" is the calculated volume of the space the TDRP occupied in the scrubber, found using the bed height and area of the scrubber cross-section. The "Predicted volume" describes the volume calculated using Eq. 25 (without the safety factor) and other experimental parameters that are listed in Appendix I.

Table 12 raises some interesting points. First, the measured volume of TDRP was always 4,000 mL because it was always measured in the same beaker, which had a capacity of 4,000 mL. This volume of TDRP almost always filled the same bed volume, which was approximately 300 mL more than was measured. The reason for the discrepancy is probably because the TDRP became more separated as it was poured into the scrubber, causing it to take up more volume. Second, the volume of TDRP predicted by the rest of the experimental parameters and results differed by up to 60%. This is most likely due to the assumptions made about the system to use Eq. 25 (width of adsorption zone is zero and constant temperature, inlet concentration, and flow rate). This large

www.manaraa.com

difference makes it difficult to accurately predict the volume of TDRP that will be actually needed, and that is why adding a safety factor of at least 3 is necessary. However, when percent differences in the last column are averaged over the six experiments, there is only a 4% average difference between the predicted volume and the volume used.

The results found in this study were compared with results from another study about different adsorbents. A study by Tsai, Jeng, & Chiang (2001) modeled the Freundlich Isotherm to experimental H_2S adsorption data of unimpregnated and impregnated activated carbons. Using the Freundlich constants found by Tsai et al., an estimated activated carbon density of 560 kg/m^3, and the same conditions used in estimating TDRP and ORM volume (flow rate and H_2S concentration), Eq. 27 can be applied to estimate the volume of unimpregnated and impregnated activated carbon needed. It was found that 1.92E-03 m^3 of unimpregnated activated carbon and 1.66E-04 m^3 of activated carbon impregnated with NaOH would be needed to remove H_2S at the WPCF for one year. If a safety factor of 3 is applied, then 5.77E-3 m^3 (5770 cm^3) of unimpregnated and 4.97E-4 m^3 (497 cm^3) of impregnated activated carbon would be needed. This is a significantly less volume of media than required for a TDRP or ORM scrubber.

A rough cost analysis can be performed to determine the minimum cost that TDRP or ORM must have to compete with unimpregnated activated carbon. A quote from Calgon Corporation (Pittsburgh, PA) for unimpregnated activated carbon was $8.44/lb. An information sheet for this type of activated carbon lists the density as 560 kg/m^3. Using the volume of unimpregnated activated carbon calculated above, the cost per year of using unimpregnated activated carbon at the WPCF would be about $60. This would mean that TDRP would have to cost $8.89/m^3 ($0.024/kg) and ORM would have to cost $4.82/m^3 ($0.019/kg) to cost the same as activated carbon. This assumes that the activated carbon is not regenerated. Impregnated activated carbon would cost more than unimpregnated activated carbon, but a cost estimate was not available.

www.manaraa.com

CHAPTER 7. CONCLUSION

Tire-derived rubber particles (TDRP) were tested at various conditions to determine optimal operating conditions for the removal of hydrogen sulfide from biogas at the Ames WPCF.

A longer empty bed contact time increased the amount of H_2S that was adsorbed up until the time of breakthrough. However, over a standard period of time that always exceeded the breakthrough time, it was seen that there was a maximum amount of H_2S was adsorbed by the media bed.

Compaction of the media bed resulted in improved H_2S adsorption capacity per unit mass of TDRP. It was hypothesized that this was due to reduced biogas short-circuiting in the scrubber. Compaction of the media bed to approximately 65% of its original volume was tested and was found to improve adsorption capacity by an average of 0.76 mg H_2S/g TDRP.

Temperature was not found to have a significant effect on the amount of H_2S that was adsorbed. Ambient temperature, around 25°C, was the most common temperature tested, but there were also tests at lower (14-20°C) and higher temperatures (44-52°C) that did not reveal a significant difference in H_2S adsorbed.

The concentration of H_2S in the biogas varied greatly over the course of the year during which the experiments were run and also during the course of individual trials. Large additions of fat, oil, and grease (FOG) caused drastic drops in H_2S concentration. It was found that the higher the H_2S loading from the inlet biogas on the media, the more H_2S was adsorbed.

Preliminary testing of siloxane concentrations in the inlet and outlet biogas from the scrubber showed that in excess of 98% of siloxanes could be removed using TDRP as the media.

Recommendations for Future Studies

The results of this study have shown that TDRP and ORM are viable materials that can be used for H_2S adsorption. However, there are still some pertinent issues that need to be addressed before this product can be commercially used.

It is important that materials currently on the market for H_2S adsorption (such as activated carbon) have the ability to be regenerated, so as to make the process more economical. No

www.manaraa.com

desorption experiments were performed during this study, so it is unknown if desorption is a possibility using TDRP or ORM. If desorption and regeneration are possible, the economics of performing this process should be compared to disposing of spent material and purchasing virgin material. As the virgin material is derived from a waste product, it may be more economic to use virgin material as opposed to regenerating the spent material.

Cost limitations during this study prevented any analysis of spent TDRP or ORM. Before this product can be commercially implemented, it is important to determine the nature of the waste being produced from the adsorption process. A Toxicity Characteristic Leaching Procedure (TCLP) should be performed to determine if the spent material is a characteristic hazardous waste. Additionally, it should be determined if the spent TDRP or ORM can be used in other applications, such as an asphalt modifier or in molded products, as virgin crumb rubber is used.

Another interesting future study could determine the effects of other components in the biogas on H_2S adsorption. Biogas contains large portions of carbon dioxide and methane, and it is possible that these compounds could interfere with adsorption onto the surface sites of the TDRP or ORM. This study would also relate to determining the adsorption mechanism of H_2S.

Perhaps the most promising results of this study relate to the ability of TDRP and ORM to remove siloxanes from biogas. The results presented in this study about siloxanes pertain mostly to some preliminary testing of siloxane concentrations in biogas. These results were extended by another researcher over the course of this study. The results of the other study confirmed that both TDRP and ORM can remove siloxanes from biogas by testing siloxane concentrations before and after the scrubber. There did not appear to be a relationship between H_2S and siloxane removal, however only two trials were tested. Additional research could focus on conditions for maximizing siloxane removal, as this study primarily focused on conditions for maximizing H_2S removal.

www.manaraa.com

REFERENCES

Abatzoglou, N. & Boivin, S. (2009). A review of biogas purification processes. *Biofuels, Bioproducts and Biorefining, 3,* 42-71.

Adib, F., Bagreev, A., & Bandosz, T. J. (2000). Analysis of the relationship between H_2S removal capacity and surface properties of unimpregnated activated carbons. *Environmental Science and Technology, 24,* 686-692.

Amari, T., Themelis, N.J., Wernick, I.K. (1999). Resource recovery from used rubber tires. *Resources Policy, 25,* 179-188.

Arizona Instrument LLC. (2005). Jerome® 860 hydrogen sulfide monitor operation manual. Retrieved December 15, 2009 from < http://www.azic.com/pdf/manual_700-0051.pdf>

American Society for Testing and Materials. (2003). Standard test method for determination of the accelerated hydrogen sulfide breakthrough capacity of granular and pelletized activated carbon."Designation: D 6646-03.

Bandosz, T. J. (2002). On the adsorption/oxidation of hydrogen sulfide on activated carbons at ambient temperatures. *Journal of Colloid and Interface Science, 246,* 1-20.

Bagreev, A. & Bandosz, T.J. (2002). A role of sodium hydroxide in the process of hydrogen sulfide adsorption/oxidation on caustic-impregnated activated carbons. *Industrial & Engineering Chemical Research, 41,* 672-679.

Bagreev, A., Katikaneni, S., Parab, S., & Bandosz, T.J. (2005). Desulfurization of digester gas: prediction of activated carbon bed performance at low concentrations of hydrogen sulfide. *Catalysis Today, 99,* 329-337.

Carnes, C. L. & Klabunde, K. J. (2002). Unique chemical reactivities of nanocrystalline metal oxides toward hydrogen sulfide. *Chemistry of Materials, 14,* 1806-1811.

Davidson, J. M., Lawrie, C. H., & Sohail, K. (1995). Kinetics of the absorption of hydrogen sulfide by high purity and doped surface area zinc oxide. *Industrial and Engineering Chemistry Research, 34,* 2981-2989.

Davis, M. & Cornwell, D. (2008). Introduction to environmental engineering. Boston, MA: McGraw-Hill.

Ellis, T. (2005). Evaluation of tire rubber particles (TDRP) for biofiltration media. *Draft final report for Envirotech Systems, Inc.*

Ellis, T., Park, J., & Oh, J. (2008). A novel and cost-effective H_2S absorption technology using tire derived rubber particles. *Submitted to IPRT Company Assistance: Grow Iowa Values Fund Seed Grant.*

www.manaraa.com

Hedden, K., Humber, L. & Rao, B.R. (1976).VDI-Bericht 253 S. 37/42. VDI-Verlag, Duesseldorf.

Keller, J. & Staudt, R. (2005). Gas adsorption equilibria: Experimental methods and adsorption isotherms. New York, NY: Springer Science and Business Media, Inc.

Kohl, A. & Nielsen, R. (1997). Gas Purification. Houston, TX: Gulf Publishing Company.

Lee, J.D., Jun, J.H., Park, N.; Ryu, S., & Lee, T. J. (2005). A study on selective oxidation of hydrogen sulfide over zeolite-NaX and-KX catalysts. *Korean Journal of Chemical Engineering*, 22, 36-41.

McBean, E. (2008). Silxanes in biogases from landfills and wastewater digesters. *Canadian Journal of Civil Engineering, 35,* 4, 431-436.

McCrady, E. (1996). Zeolites. *Conservation OnLine: Abbey Newsletter.* 20 (7), Dec. 1996. <http://palimpsest.stanford.edu/byorg/abbey/an/an20/an20-7/an20-702.html>

McKinsey Zicarai, S. (2003). Removal of hydrogen sulfide from biogas using cow-manure compost. *Thesis Presented to the Faculty of the Graduate School of Cornell University,* 1-104.

Nagl, G. (1997). Controlling H_2S emissions. *Chemical Engineering, 104(3),* 125-131.

Osorio, F. & Torres, J.C. (2009). Biogas purification from anaerobic digestion in a wastewater treatment plant for biofuel production. *Renewable Energy, 34*, 2164-2171.

Rodriguez, J.A. & Maiti, A. (2000). Adsorption and decomposition of H_2S on MgO(100), NiMgO(100), and ZnO(0001) surfaces: A first-principles density functional study. *Journal of Physical Chemistry B, 104,* 3630-3638.

Saeed, S., Kao, S., & Graening, G. (2002). Comparison of impinge and canister methods for the determination of siloxanes in air. *Presented at the AWMA Symposium on Air Quality Measurement methods and Technology in San Francisco, CA.* Retrieved January 15, 2010 from < http://www.airtoxics.com/literature/papers/Siloxanes_Paper_AWMA.pdf>

Sunthonpagasit, N. & Duffey, M.R. (2004). Scrap tires to crumb rubber: Feasibility Analysis for Processing Facilities. *Resources Conservation & Recycling,40,* 281-299.

Trapezoidal Rule. (2010). In *Wikipedia, the free encyclopedia.* Retrieved February 1, 2010 from <http://en.wikipedia.org/wiki/Trapezoidal_rule>

Truong, L.V.-A. & Abatzoglou, N. (2005). A H_2S reactive adsorption process for the purification of biogas prior to its use as a bioenergy vector. *Biomass and Bioenergy, 29*, 142-151.

Tsai, J., Jeng, F., Chiang, H. (2001). Removal of H_2S from exhaust gas by use of alkaline activated carbon. *Adsorption, 7,* 357-366.

www.manaraa.com

U.S. Environmental Protection Agency. (2009). Ground Rubber Applications. Retrieved November 23, 2009 from <http://www.epa.gov/osw/conserve/materials/tires/ground.htm>

U.S. Environmental Protection Agency. (2003). Toxicological Review of Hydrogen Sulfide (CAS No. 7783-06-4). Retrieved September 23, 2009 from <http://www.epa.gov/ncea/iris/toxreviews/0061-tr.pdf>

Wang, X., Ma, X., Xu, X., Sun, L., & Song, C. (2008). Mesoporous-molecular-sieve-supported polymer sorbents for removing H_2S from hydrogen gas streams. *Topics in Catalysis, 49,* 108-117.

Wark, K., Warner, C., & Davis, W. (1998). Air pollution: Its origin and control. Menlo Park, CA: Addison Wesley Longman.

Wheeler, P., Jaatinen, T., Lindberg, A., Holm-Nielsen, J.B., Wellinger, A., & Pettigrew, A. (2000). Biogas Upgrading and Utilisation. *IEA Bioenergy Task 24.* International Energy Association, Paris, France.

Yan, R., Chin, T., Ng, Y.L., Duan, H., Liang, D.T., & Tay, J.H. (2004). Influence of surface properties on the mechanism of H_2S removal by alkaline activated carbons. *Environmental Science & Technology, 38,* 316-323.

Yuan, W. & Bandosz, T.J. (2007). Removal of hydrogen sulfide from biogas on sludge-derived adsorbents. *Fuel, 86,* 2736-2746.

Xiao, Y., Wang, S., Wu, D., & Yuan, Q. (2008). Experimental and simulation study of hydrogen sulfide adsorption on impregnated activated carbon under anaerobic conditions. *Journal of Hazardous Materials, 153,* 1193-1200.

www.manaraa.com

APPENDIX I: HYDROGEN SULFIDE TESTING RESULTS

Empty Bed Contact Time

Table 13 lists the complete data for each trial used to evaluate the effect of empty bed contact time on H_2S adsorption by TDRP.

Table 13, Raw data for empty bed contact time effects

	Trial 7	Trial 8	Trial 9	Trial 10	Trial 26	Trial 27
Mass of TDRP, g	1420	1500	1420	1500	1580	1580
Vol of TDRP, mL	4000	4000	4000	4000	4000	4000
Avg Flow Rate, L/min	3.13	2.09	3.13	3.13	1.04	0.52
Total Adsorbed, mg H_2S/g TDRP	1.19	1.29	1.09	1.13	1.09	1.10
Adsorbed at breakthrough, mg H_2S/g TDRP	0.49	0.86	0.39	0.51	0.67	1.09
Time until breakthrough, min	794	2002	779	903	2046	3524
Empty bed contact time, s	81.48	134.57	83.23	83.23	256.42	483.30
H_2S Sensor inlet temp, C	28.4	24	24.7	28.3	22.7	23.1
H_2S Sensor outlet temp, C	28.4	24	24.7	28.1	22.8	23.1
Temp avg, C (temp probe in scrubber)	28.8	25.5	25.4	28.7	23.1	24.0
Temp stdev, C (temp probe in scrubber)	1.4	3.7	2.8	2.3	6.5	1.8
Temp Dial Avg, C					27.1	24
mg H_2S/g TDRP/hr from inlet	0.0390	0.0281	0.0377	0.0389	0.0246	0.0216
Average outlet H_2S conc before breakthrough	9.0	12.1	6.9	7.8	28.9	100.9
Stdev outlet H_2S conc before breakthrough	5.6	4.8	2.2	3.7	11.3	29.7
Average inlet H_2S conc before breakthrough	220.0	233.1	184.1	217.6	390.9	772.3
Stdev inlet H_2S conc before breakthrough	6.0	11.6	11.2	21.0	43.1	38.8

Temperature

Table 14 lists the complete data for each trial used to evaluate the effect of low temperature on H_2S adsorption by TDRP. It should be noted that for Trials 22 and 30, the data logging thermocouple was malfunctioning so a dial thermometer was installed in the scrubber and manual readings were taken four times over the course of the trial and averaged.

www.manaraa.com

Table 14, Raw data for low temperature effect

	Trial 16	Trial 22	Trial 30
Mass of TDRP, g	1161	1420	1640
Vol of TDRP, mL	4000	4000	4000
Avg Flow Rate, L/min	2.6	3.13	3.13
Total Adsorbed, mg H_2S/g TDRP	3.01	3.51	3.66
Adsorbed at breakthrough, mg H_2S/g TDRP	0.56	2.31	0.13
Time until breakthrough, min	401	1621	124
Empty bed contact time, s	96.70	81.12	83.37
H_2S Sensor inlet temp, C	33.2	25.2	16.0
H_2S Sensor outlet temp, C	33.2	25.2	16.0
Temp avg, C (temp probe in scrubber)	16.9		
Temp stdev, C (temp probe in scrubber)	5.6	13.7	8.9
Temp Dial Avg, C		20.7	14.2
mg H_2S/g TDRP/hr from inlet	0.0905	0.0850	0.2021
Average outlet H_2S conc before breakthrough	33.8	24.77	58.04
Stdev outlet H_2S conc before breakthrough	8.5	5.69	17.10
Average inlet H_2S conc before breakthrough	533.2	505.16	874.87
Stdev inlet H_2S conc before breakthrough	60.8	39.36	24.47

Table 15 lists the complete data for each trial used to evaluate the effect of medium temperature on H_2S adsorption by TDRP. It should be noted that for Trial 23 the data logging thermocouple was malfunctioning and the temperature used was taken from the dial thermometer in the scrubber.

www.manaraa.com

Table 15, Raw data for medium temperature effect

	Trial 7	Trial 8	Trial 9	Trial 10	Trial 23	Trial 26	Trial 27	Trial 34
Mass of TDRP, g	1420	1500	1420	1500	1380	1580	1580	1620
Vol of TDRP, mL	4000	4000	4000	4000	4000	4000	4000	4000
Avg Flow Rate, L/min	3.1	2.1	3.1	3.1	3.13	1.04	0.52	3.13
Total Adsorbed, mg H_2S/g TDRP	1.19	1.29	1.09	1.13	5.19	1.09	1.10	0.49
Adsorbed at breakthrough, mg H_2S/g TDRP	0.49	0.86	0.39	0.51	2.05	0.67	1.09	0.16
Time until breakthrough, min	794	2002	779	903	1034	2046	3524	459
Empty bed contact time, s	81.48	134.57	83.23	83.23	81.85	256.42	483.3	83.37
H_2S Sensor inlet temp, C	28.4	24	24.7	28.3	22.82	22.70	23.09	24.18
H_2S Sensor outlet temp, C	28.4	24	24.7	28.1	22.82	22.76	23.11	24.20
Temp avg, C (temp probe in scrubber)	28.8	25.5	25.4	28.7		23.05	23.98	25.19
Temp stdev, C (temp probe in scrubber)	1.4	3.7	2.8	2.3	9.4	6.50	1.81	1.09
Temp Dial Avg, C					26.4	27.1	24	27.5
mg H_2S/g TDRP/hr from inlet	0.0390	0.0281	0.0377	0.0389	0.2180	0.0246	0.0216	0.0296
Average outlet H_2S conc before breakthrough	9.0	12.1	6.9	7.8	34.00	28.93	100.86	19.05
Stdev outlet H_2S conc before breakthrough	5.6	4.8	2.2	3.7	6.70	11.26	29.66	2.13
Average inlet H_2S conc before breakthrough	220.0	233.1	184.1	217.6	664.97	390.95	772.27	159.46
Stdev inlet H_2S conc before breakthrough	6.0	11.6	11.2	21.0	46.13	43.12	38.77	2.77

المنارة للاستشارات
www.manaraa.com

Table 16 lists the complete data for each trial used to evaluate the effect of high temperature on H_2S adsorption by TDRP. It should be noted that for Trial 21 the data logging thermocouple was malfunctioning and the temperature used was taken from the dial thermometer in the scrubber.

Table 16, Raw data for high temperature effect

	Trial 18	Trial 21	Trial 28
Mass of TDRP, g	1260	1460	1660
Vol of TDRP, mL	4000	4000	4000
Avg Flow Rate, L/min	3.1	3.13	3.13
Total Adsorbed, mg H_2S/g TDRP	3.14	1.71	1.97
Adsorbed at breakthrough, mg H_2S/g TDRP	2.48	1.18	0.90
Time until breakthrough, min	1961	1944	678
Empty bed contact time, s	80.6	84.33	83.37
H_2S Sensor inlet temp, C	33.9	23.8	19.50
H_2S Sensor outlet temp, C	33.9	23.78	19.49
Temp avg, C (temp probe in scrubber)	52.4		52.41
Temp stdev, C (temp probe in scrubber)	4.3	13.8	5.40
Temp Dial Avg, C		43.9	41.5
mg H_2S/g TDRP/hr from inlet	0.0868	0.0408	0.1070
Average outlet H_2S conc before breakthrough	32	11.18	33.08
Stdev outlet H_2S conc before breakthrough	8.7	2.49	6.71
Average inlet H_2S conc before breakthrough	415.9	217.59	547.43
Stdev inlet H_2S conc before breakthrough	31.8	20.54	5.55

Compaction

Table 17 lists complete data for each trial with no compaction that was used to compare to trials with compaction. These trials were chosen because of similar operational conditions to those trials with compaction. Table 18 lists complete data for each trial with compaction. The amount of compaction is reflected in volume of TDRP. Each of these trials started with a 4,000 mL bed, but was manually compacted to the volume specified in Table 18.

www.manaraa.com

Table 17, Raw data for trials with no compaction

	Trial 7	Trial 9	Trial 10
Mass of TDRP, g	1420	1420	1500
Vol of TDRP, mL	4000	4000	4000
Avg Flow Rate, L/min	3.1	3.1	3.1
Total Adsorbed, mg H_2S/g TDRP	1.19	1.09	1.13
Adsorbed at breakthrough, mg H_2S/g TDRP	0.49	0.39	0.51
Time until breakthrough, min	794	779	903
Empty bed contact time, s	81.48	83.23	83.23
H_2S Sensor inlet temp, C	28.4	24.7	28.3
H_2S Sensor outlet temp, C	28.4	24.7	28.1
Temp avg, C (temp probe in scrubber)	28.8	25.4	28.7
Temp stdev, C (temp probe in scrubber)	1.4	2.8	2.3
Temp Dial Avg, C			
mg H_2S/g TDRP/hr from inlet	0.0390	0.0377	0.0389
Average outlet H_2S conc before breakthrough	9.0	6.9	7.8
Stdev outlet H_2S conc before breakthrough	5.6	2.2	3.7
Average inlet H_2S conc before breakthrough	220.0	184.1	217.6
Stdev inlet H_2S conc before breakthrough	6.0	11.2	21.0

Table 18, Raw data for trials with compaction

	Trial 11	Trial 12	Trial 13	Trial 14
Mass of TDRP, g	1580	1440	1462	1378
Vol of TDRP, mL	2600	2680	2880	2640
Avg Flow Rate, L/min	3.1	3.1	3.5	2.6
Total Adsorbed, mg H_2S/g TDRP	1.49	1.61	1.98	2.49
Adsorbed at breakthrough, mg H_2S/g TDRP	0.77	0.62	0.87	1.74
Time until breakthrough, min	1001	807	909	2099
Empty bed contact time, s	60	56.13	53.14	65.77
H2S Sensor inlet temp, C	24.9	27	27.6	28.1
H2S Sensor outlet temp, C	24.9	27.1	27.6	28.1
Temp avg, C (temp probe in scrubber)	25.3	26.0		26.3
Temp stdev, C (temp probe in scrubber)	1.6	3.5		4.7
Temp Dial Avg, C				
mg H_2S/g TDRP/hr from inlet	0.0527	0.0520	0.0697	0.0533
Average outlet H_2S conc before breakthrough	14.6	15.8	14.6	23.1
Stdev outlet H_2S conc before breakthrough	6.8	2.1	6.1	5.8
Average inlet H_2S conc before breakthrough	300.0	273.6	327.6	352.3
Stdev inlet H_2S conc before breakthrough	13.6	8.5	16.9	21.4

www.manaraa.com

Mass of Media Bed

The effect of the mass of the media bed on H_2S adsorption by TDRP was determined by comparing a full bed, defined as 4,000 mL, to a half bed, defined as 2,000 mL. Table 19 lists complete data for the full bed trials that were compared to the half bed trials listed in Table 20. The trials in Table 19 were selected out of all the trials that used a full bed because they had the most similar operational conditions to the half bed trials in Table 20.

Table 19, Raw data for full bed TDRP mass

	Trial 1	Trial 2
Mass of TDRP, g	1340	1340
Vol of TDRP, mL	4000	4000
Avg Flow Rate, L/min	5	4.9
Total Adsorbed, mg H_2S/g TDRP	3.24	2.42
Adsorbed at breakthrough, mg H_2S/g TDRP	2.72	1.69
Time until breakthrough, min	1465	1269
Empty bed contact time, s	50.52	51.55
H_2S Sensor inlet temp, C	27.6	27.5
H_2S Sensor outlet temp, C	27.4	27.4
Temp avg, C (temp probe in scrubber)	26.9	27.3
Temp stdev, C (temp probe in scrubber)	1.8	1.9
Temp Dial Avg, C		
mg H_2S/g TDRP/hr from inlet	0.1090	0.0860
Average outlet H_2S conc before breakthrough	136.0	4.6
Stdev outlet H_2S conc before breakthrough	14.8	10.7
Average inlet H_2S conc before breakthrough	370.9	289.1
Stdev inlet H_2S conc before breakthrough	18.7	3.7

www.manaraa.com

Table 20, Raw data for half bed TDRP mass

	Trial 5	Trial 6
Mass of TDRP, g	670	670
Vol of TDRP, mL	2000	2000
Avg Flow Rate, L/min	5.1	5.2
Total Adsorbed, mg H_2S/g TDRP	1.17	1.22
Adsorbed at breakthrough, mg H_2S/g TDRP	0.14	0.28
Time until breakthrough, min	100	136
Empty bed contact time, s	24.71	24.23
H_2S Sensor inlet temp, C	26.9	26.1
H_2S Sensor outlet temp, C	27	26.1
Temp avg, C (temp probe in scrubber)	26.4	26.6
Temp stdev, C (temp probe in scrubber)	3.7	7.2
Temp Dial Avg, C		
mg H_2S/g TDRP/hr from inlet	0.1714	0.1550
Average outlet H_2S conc before breakthrough	46.7	33.3
Stdev outlet H_2S conc before breakthrough	49.7	34.5
Average inlet H_2S conc before breakthrough	274.3	248.9
Stdev inlet H_2S conc before breakthrough	6.5	7.2

Comparison to Other Adsorbents

Steel wool and glass beads were used in the scrubber system to serve as a comparison to TDRP and ORM. The results can be seen in Table 21.

www.manaraa.com

Table 21, Raw data for trials with steel wool and glass beads

	Trial 37	Trial 38	Trial 39
Mass of TDRP, g	120	280	6640
Vol of TDRP, mL	4000	4000	4000
Avg Flow Rate, L/min	2.6	1.0	1.0
Total Adsorbed, mg H_2S/g TDRP	0.71	0.17	0.07
Adsorbed at breakthrough, mg H_2S/g TDRP			
Time until breakthrough, min			
Empty bed contact time, s	96.53	244.5	253.16
H_2S Sensor inlet temp, C	14.0	11.7	15.4
H_2S Sensor outlet temp, C	14.0	11.7	15.3
Temp avg, C (temp probe in scrubber)	14.3	21.3	15.3
Temp stdev, C (temp probe in scrubber)	7.3	1.8	3.6
Temp Dial Avg, C	20.8	21.5	22.2
mg H_2S/g TDRP/hr from inlet	0.2351	0.0485	0.0035
Average outlet H_2S conc before breakthrough			
Stdev outlet H_2S conc before breakthrough			
Average inlet H_2S conc before breakthrough			
Stdev inlet H_2S conc before breakthrough			
Material	Steel wool	Steel wool	Glass beads

Isotherm Modeling

Experimental data was fit to the Freundlich Isotherm model. Measured and converted values are shown in Table 22 and Table 23 for use in the Freundlich Isotherm for ORM and TDRP at 25°C. Data used for finding the "low temperature" isotherm for TDRP at 14-20°C and the "high temperature" isotherm for TDRP at 44-52°C can be found in Table 24 and Table 25, respectively. Table 26 through Table 29 show values used to model the Langmuir Isotherm.

www.manaraa.com

Table 22, Raw and converted data used to find Freundlich constants for ORM at 25°C

Trial	Avg Inlet H_2S Conc, ppm	Adsorbed at breakthrough, mg H_2S/g TDRP	Temp, C	C_e, kg H_2S/m^3	X_{sat}, kg H_2S/kg TDRP	log(C_e)	log(X_{sat})
31	785.25	1.95	24.66	1.09E-03	1.95E-03	-2.96	-2.71
32	722.97	1.00	28.86	1.00E-03	9.98E-04	-3.00	-3.00
33	240.99	0.36	25.64	3.35E-04	3.64E-04	-3.47	-3.44
35	122.37	0.38	24.77	1.70E-04	3.79E-04	-3.77	-3.42
36	108.73	0.32	24.20	1.51E-04	3.22E-04	-3.82	-3.49

Table 23, Raw and converted data used to find Freundlich constants for TDRP at 25°C

Trial	Avg Inlet H_2S Conc, ppm	Adsorbed at breakthrough, mg H_2S/g TDRP	Temp, C	C_e, kg H_2S/m^3	X_{sat}, kg H_2S/kg TDRP	log(C_e)	log(X_{sat})
7	219.99	0.49	28.77	3.06E-04	4.92E-04	-3.51	-3.31
8	233.07	0.86	25.50	3.24E-04	8.57E-04	-3.49	-3.07
9	184.13	0.39	25.36	2.56E-04	3.91E-04	-3.59	-3.41
10	217.61	0.51	28.68	3.02E-04	5.05E-04	-3.52	-3.30
23	664.97	2.05	26.40	9.24E-04	2.05E-03	-3.03	-2.69
34	159.46	0.16	25.19	2.22E-04	1.60E-04	-3.65	-3.79

Table 24, Raw and converted data used to find Freundlich constants for TDRP at 14-20°C (low temperature)

Trial	Avg Inlet H_2S Conc, ppm	Adsorbed at breakthrough, mg H_2S/g TDRP	Temp, C	C_e, kg H_2S/m^3	X_{sat}, kg H_2S/kg TDRP	log(Ce)	log(Xsat)
16	533.20	0.56	16.90	7.62E-04	5.56E-04	-3.12	-3.26
22	505.16	2.31	20.70	7.22E-04	2.31E-03	-3.14	-2.64
30	874.87	0.13	14.20	1.25E-03	1.27E-04	-2.90	-3.90

www.manaraa.com

Table 25, Raw and converted data used to find Freundlich constants for TDRP at 44-52°C (high temperature)

Trial	Avg Inlet H_2S Conc, ppm	Adsorbed at breakthrough, mg H_2S/g TDRP	Temp, C	C_e, kg H_2S/m^3	X_{sat}, kg H_2S/kg TDRP	log(Ce)	log(Xsat)
18	415.90	2.48	52.40	5.32E-04	2.48E-03	-3.27	-2.61
21	217.59	1.18	43.90	2.79E-04	1.18E-03	-3.56	-2.93
28	547.43	0.90	52.41	7.01E-04	9.02E-04	-3.15	-3.04

Table 26, Raw and converted data used to fit Langmuir Isotherm for ORM at 25°C

Trial	Avg Inlet H_2S Conc, ppm	Adsorbed at breakthrough, mg H_2S/g TDRP	Temp, C	C_g, g/m^3	W, kg H_2S/kg TDRP	C_g/W
31	785.25	1.95	24.66	1.09	1.95E-03	559.30
32	722.97	1.00	28.86	1.00	9.98E-04	1007.15
33	240.99	0.36	25.64	0.33	3.64E-04	920.30
35	122.37	0.38	24.77	0.17	3.79E-04	449.28
36	108.73	0.32	24.20	0.15	3.22E-04	469.79

Table 27, Raw and converted data used to fit Langmuir Isotherm for TDRP at 25°C

Trial	Avg Inlet H_2S Conc, ppm	Adsorbed at breakthrough, mg H_2S/g TDRP	Temp, C	C_g, g/m^3	W, kg H_2S/kg TDRP	C_g/W
7	219.99	0.49	28.77	0.31	4.92E-04	621.72
8	233.07	0.86	25.50	0.32	8.57E-04	378.12
9	184.13	0.39	25.36	0.26	3.91E-04	654.79
10	217.61	0.51	28.68	0.30	5.05E-04	598.44
23	664.97	2.05	26.40	0.92	2.05E-03	450.88
34	159.46	0.16	25.19	0.22	1.60E-04	1381.38

www.manaraa.com

Table 28, Raw and converted data used to fit Langmuir Isotherm for TDRP at 14-20°C (low temperature)

Trial	Avg Inlet H_2S Conc, ppm	Adsorbed at breakthrough, mg H_2S/g TDRP	Temp, C	C_g, g/m^3	W, kg H_2S/kg TDRP	C_g/W
16	533.20	0.56	16.90	0.76	5.56E-04	1372.43
22	505.16	2.31	20.70	0.72	2.31E-03	312.72
30	874.87	0.13	14.20	1.25	1.27E-04	9870.72

Table 29, Raw and converted data used to fit Langmuir Isotherm for TDRP at 44-52°C (high temperature)

Trial	Avg Inlet H_2S Conc, ppm	Adsorbed at breakthrough, mg H_2S/g TDRP	Temp, C	C_g, g/m^3	W, kg H_2S/kg TDRP	C_g/W
18	415.90	2.48	52.40	0.53	2.48E-03	214.42
21	217.59	1.18	43.90	0.28	1.18E-03	236.03
28	547.43	0.90	52.41	0.70	9.02E-04	776.58

Table 30, Raw data to compare actual and predicted volumes of TDRP

Trial	Ce, kg/m^3	Volume, mL	ρ_{ad}, kg/m^3	Mass flow rate, kg/s	V_{ad}, m/s	D_b, m	t_B, min	Predicted Volume, mL
7	3.06E-04	4000	8.36E-05	5.68E-05	1.07E-05	0.4207	794	4765
8	3.24E-04	4000	8.86E-05	3.79E-05	6.42E-06	0.4207	2002	7233
9	2.56E-04	4000	7.00E-05	5.68E-05	1.24E-05	0.4207	779	5434
10	3.02E-04	4000	8.27E-05	5.68E-05	1.02E-05	0.4207	903	5177
23	9.24E-04	4000	2.53E-04	5.68E-05	4.3E-06	0.427	1034	2506
34	2.22E-04	4000	6.05953E-05	5.68E-05	1.23E-05	0.4349	459	3170

www.manaraa.com

APPENDIX II: SILOXANE SAMPLING PROTOCOL

The following instruments and chemicals were used in sample collection:

- SKC 222 Series pump × 2
- Impinger ×4
- 20ml midget impingers
- Cooler
- Tubing
- Methanol (Analytical grade)
- Ice

Figure 31 shows the sampling system flow diagram with equipment and methanol in place.

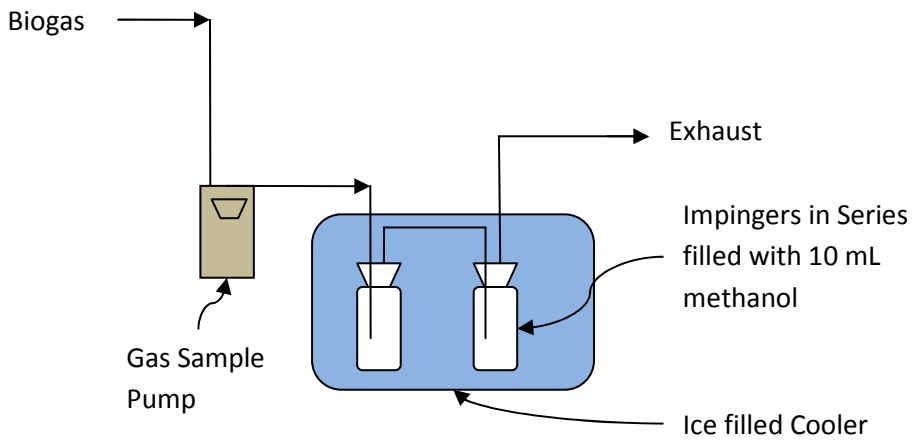

Figure 31, Siloxane sampling system

First, the gas sample pump flow rate was adjusted close to 110-120mL/min before sampling. Next, the instruments were connected as shown in Figure 31. Ten milliliters of methanol was added to each impinger. Before connecting the pumps to the impingers they were run for several minutes to pump out residue air. After air was purged through the system, the pump was stopped and the counter total recorded.

After checking the entire connection, the pumps were started and siloxane samples were collected. Sampling start time was recorded. A sample was collected for three hours. The system was checked at least once per hour. After the three hour sample time was complete, the pumps were stopped, and the time and counter position was recorded. The total biogas amount

www.manaraa.com

transferred by each pump was calculated by the difference between start and stop numbers (one count equals the calibration volume). The flow rate was determined by dividing the biogas volume by the time difference.

After the sampling system was dismantled, methanol was added to each impinger to maintain a volume of 10 mL. Then, the methanol was transferred to marked vials with gas tight covers and a seal to minimize volatilization. Vials were kept near 4°C prior to GC/MS analysis.

The GC/MS sampling system consisted of the following setup:

- Gas Chromatography System : Varian 3900
- Carrier gas: helium
- Head pressure 1ml/min constant flow
- Capillary columns Varian VF-5MS, 30M x 0.25mm, DF=0.25
- Temperature program 40 C (6min), 3C/min to 100 C (0min), 20C/min to 250C (15min)
- Oven temp: 210 °C
- Mass Spectrometer: Varian 2000
- Activation EI
- Transfer line temperature: 280 °C
- Mass window: 60m/z-400m/z
- Modus: scan
- Scans: 1.37/s
- Varian 8410 Autosampler

An external calibration curve was used to establish the baseline concentrations of siloxane samples. Five different concentrations of siloxane standard samples were used to develop the curve. Before each test, the external calibration curve was performed to ensure accuracy. The collected samples were transferred to the GC/MS autosampler vials. Five standard samples and collected samples were all placed on the autosampler of GC/MS. After analysis by the GC/MS, the siloxane concentration in methanol was established, and the final gas concentration was back-calculated with biogas and methanol volume.

Siloxane methanol concentration × 10 mL / biogas volume = final result

www.manaraa.com

ACKNOWLEDGEMENTS

I would like to extend my gratitude and appreciation to those who made this research possible and who helped me along the way. Thank you to Dr. Eric Evans, who was both an invaluable resource to me on this project and an integral part of teaching me about research and environmental engineering. Thank you to Dr. Tim Ellis for serving as my major professor and offering guidance on this project. Thank you to Dr. Hans van Leeuwen and Dr. Hogan Martin for serving on my POS committee, offering suggestions, and taking interest in my project. Thank you to Jim McElvogue and all the operators and staff at the Ames Water Pollution Control Facility for their cooperation and assistance throughout the course of this study. Thank you to Ross Tuttle for running the experiments and collecting data during summer 2009 so that I could pursue an internship opportunity. Finally, thank you to my family and friends for being supportive of me every step of the way!

www.manaraa.com